Spring 4-19-2013

Evaluation of Statistical Energy Analysis for Prediction of Breakout Noise from Air Duct

Himanshu S. Malushte
University of Nebraska-Lincoln, hmalushte@unomaha.edu

Follow this and additional works at: http://digitalcommons.unl.edu/archengdiss

EVALUATION OF STATISTICAL ENERGY ANALYSIS FOR PREDICTION OF BREAKOUT NOISE FROM AIR DUCT

by

Himanshu S. Malushte

A THESIS

Presented to the Faculty of

The Graduate College at the University of Nebraska

In Partial Fulfillment of Requirements

For the Degree of Master of Science

Major: Architectural Engineering

Under the Supervision of Professor Siu-Kit Lau

Lincoln, Nebraska

May, 2013

EVALUATION OF STATISTICAL ENERGY ANALYSIS FOR PREDICTION OF BREAKOUT NOISE FROM AIR DUCT

Himanshu S. Malushte, M.S.

University of Nebraska, 2013

Advisor: Siu-Kit Lau

The breakout noise from an air-conditioning duct is of immense concern in order to maintain a sound environment at home, office spaces, hospitals, etc. The challenge lies in correctly estimating the breakout noise by knowing the breakout sound transmission loss from the air duct. The ASHRAE Handbook: HVAC Applications (ASHRAE, 2011) currently lists some of theoretical transmission loss values for limited duct dimensions and gages (duct-wall thickness) at the octave band frequencies. Statistical Energy Analysis (SEA) is promising to predict the sound transmission loss for breakout noise for any given air duct configuration, particularly at high frequency. Though there are deterministic approaches such as finite element method (FEM) and boundary element method (BEM), they are unable to yield results efficiently for high frequency, while they also demand long computational time and memory. SEA on the contrary saves the computational effort and thus computational time. In this study, theoretical transmission loss of random duct configuration is selected from ASHRAE Handbook: HVAC Applications (ASHRAE, 2011) to evaluate the SEA method for correctly predicting the breakout sound transmission noise. All the applicable parameters for implementing SEA on a duct are discussed and the method is then simulated. The predicted results are then compared with the theoretical results (ASHRAE, 2011). Initially, there are some discrepancies between the

predicted results by SEA and the theoretical results in transmission loss observed at higher frequencies. Further investigation leads to a formulation of a factor that is applied to the conventional SEA approach. The predicted results from the new formulation show a close agreement with the existing theoretical results and are mostly within 3 dB difference. The SEA predictions are also compared with the experimental data (Cummings 1983a) to establish SEA's validity. The SEA predicted results are also found to be close with the experimental results for the all the duct configurations and maintain agreement mostly within 3 dB.

Acknowledgements

This research has been a unique experience. It compelled me to step out of the familiar science of investigating a problem by the conventional methods in order to suggest an alternate technique to address the same problem more effectively. This research at times has been mercurial in terms of the behavior of the problem associated to yield any logical results. This challenged me even further to thoroughly investigate each and every parameter associated with the study and deduce a compatible approach to address the problem. In the process I would like to thank my advisor Dr. Siu-Kit Lau who has been aplomb throughout my study especially in times of inconclusive study output and thereby directing me to a more practical approach. I am grateful to the university library resource database that gave me an access to the numerous scientific research articles published over the time in my related research field.

Finally, I may not be able to close my acknowledgements without making a mention of my fellow graduate student Carl Hart for his valuable feedback on my research from time to time and for ceaselessly sharing his expertise in the field of structural acoustics. I would also like to take an opportunity to thank my examining committee members Dr. Lily Wang and Dr. Yuebin Yu for accepting my invitation to be on my committee on such a short notice and giving their valuable advice on this research.

Table of Contents

List of Figures

List of Tables

List of Symbols

Lower case letters

a, b Cross sectional dimensions of the duct

f Frequency

f_c Critical frequency

f_{11} First vibration resonant frequency of the duct wall

c Speed of sound

c_B Bending wave speed

c_L Longitudinal wave speed

h Thickness of the duct wall

k Wavenumber

l_1, l_2 Dimensions of duct wall

n Modal density

v Average vibration velocity

Upper case letters

B Bending stiffness

E Young's modulus

E_i Energy in Subsystem i

L^* Effective length of the duct

P Total length of the edges of the duct walls

P_l Perimeter of the duct wall

R Sound reduction index

S Total surface area of the duct walls

S^* Effective surface area of the duct

S_a Surface area of the internal air cavity

S_l Surface area of a single duct wall

V Enclosed air volume in the duct

W Sound power

Greek notations

α Duct Attenuation Rate

μ Poisson's ratio

ρ Density of the duct material

ρ_0 Density of air

ρ_s Surface density of the duct wall

γ Absorption coefficient of the duct wall

η_{11} Internal loss factor of the enclosed space

η_{ij} Coupling loss factor from subsystem i to j

η_s Dissipation loss factor of the duct wall

σ Radiation efficiency

τ Transmission coefficient

Chapter 1: Introduction

The objective of this study is to evaluate the Statistical Energy Analysis (SEA) method for prediction of the Transmission Loss (TL) of breakout noise through air duct walls for any given dimension of an air duct. This SEA method will be evaluated by comparing the SEA predicted results to the theoretical data published for the corresponding configurations of air ducts from ASHRAE Handbook: HVAC Applications (ASHRAE, 2011). The predicted results will also be compared with the experimental data (Cummings, 1983a) published for validation. As the finite element method (FEM) or boundary element method (BEM) are ineffective at the higher frequencies, the SEA is assumed to serve as a useful tool for engineering design. The evaluation of this approach will be further stretched to its application on air ducts with different dimension, different duct materials and different gages (i.e. duct wall thickness).

1.1 Analysis of Background of Statistical Energy

Statistical Energy Analysis (SEA) is a probabilistic analysis tool to determine the global vibrational energies of complicated systems. The development of Statistical Energy Analysis (SEA) emerged to predict the vibrational response to rocket noise of satellite launch vehicles and their payloads in the early 1960's (Heckl and Lewit, 1994). Though the vibrational modes of structures could to be predicted computationally, the size of the models and the computational speed was discouraging to the engineers as it could predict only a few of the lowest order modes. Traditionally, in analysis of mechanical vibrations, the lowest modes are usually of most interest because these modes tend to produce the greatest displacement response. But while designing

large and lightweight structures, it is imperative to account for high frequency broadband loads to predict fatigue, failure or noise emission. The SEA proves to be an effective method to predict high frequency loads. Since its formulation, SEA has been widely used in a growing number of applications. It has also been successful in predicting the average vibrational amplitudes and sound pressures in space vehicles, airplanes, ships, buildings, large machines, etc. (Heckl and Lewit, 1994)

1.2 Approach of Statistical Energy Analysis

To start with, the abbreviation "SEA" exhibits its methodology. 'Statistical' corresponds to the systems being studied, which are assumed to be taken from a statistical population having known distributions of their dynamical parameters. The 'Energy' describes the behavior of the system in terms of stored, dissipated and exchanged energies of acoustics and/or vibration. 'Analysis' represents that SEA is a framework rather than a specific technique (Lyon and DeJong, 1995). The approach of SEA is to break up the given system into subsystems. Subsystems are a division of several physical elements so that the vibro-acoustic characteristics are similar over them like damping, excitation and coupling properties. SEA then models the entire system and the energy distribution over the subsystems with the help *power balance equations*. The underlying assumption is that total incoming power and total dissipated power are equal. Besides the power balance assumption, there are two other important assumptions in the conventional SEA, with regard to the damping: (1) the damping is proportional to the kinetic energy of a subsystem and (2) the rate of power flow between subsystems is proportional to the difference in subsystem energies (Woodhouse, 1981 b). Certain transmission coefficients need to be evaluated in order to understand the relation of transferred power between the subsystems to their equilibrium

energies. These coefficients can be estimated by one of the main approaches in SEA: (1) the modal approach, (2) the wave approach and (3) the mobility approach. The modal approach controls the interaction of the uncoupled modes in the subsystems. With the decoupled boundary condition, it is possible to express the multimode power transfer coefficients. This is an ideal approach for vibro-acoustic problems involving acoustic interaction between enclosed volumes, but it is not the ideal approach for coupling between solid structures. To overcome that problem, the wave approach plays an important role. The vibrational fields in this approach are modeled as superposition of the travelling waves and the transferred power within the subsystems can be derived from the wave transmission and reflections at the subsystem interfaces. The mobility approach is based on the concept of dynamic mobility, or impedance to express the interaction of the coupled subsystems (Fahy, 1994). In this study, the wave approach will be employed for the coupling between the structures. This method is largely standardized and commonly used by the engineers.

1.3 Important Parameters in Statistical Energy Analysis

There are four essential parameters in the study of SEA: (1) the damping loss factor, (2) the coupling loss factor, (3) the power (input, dissipated, transmitted) and (4) number of modes per frequency band. The damping loss factor relates to the power dissipated in a subsystem. To experimentally determine the damping loss factor, it needs to be spatially averaged for each frequency band. The damping loss factor can be measured by various methods, for instance, the power injection method that is performed by applying a known power input. The coupling loss factor relates to the energy flow between subsystems. It is defined as the fraction of energy that is transmitted from one subsystem to another (Craik, 1996). While dealing with structures, the

coupling loss factor is proportional to the transmission coefficient that depends upon the orientation, thickness and material properties of the structure. In acoustics, the coupling loss factor is proportional to the radiation efficiency. To experimentally determine the coupling loss factor within the subsystems, one of the subsystems should be more damped than the other. The damping loss factor of the other subsystem should be known. One of the subsystems is directly excited during the experiment. The reaction of both the subsystems must be evaluated to determine the energy in each subsystem. The power flow from one subsystem to another can be evaluated once you calculate all the loss factors which are dependent on the dimensions, material properties of the subsystems, and the energy transfer from one to another. The net power flow can then be calculated knowing the individual power flows for all subsystems. The fourth parameter is the number of modes per frequency band as mentioned, that is the number of modes per the evaluated frequency band valid for both, the constant bandwidth and the octave band. Modal density is another important parameter which emerges stating the number of modes per frequency bandwidth.

1.4 Some Limitations and Assumptions in Statistical Energy Analysis

SEA has limitation in accuracy at the lower frequency ranges, generally below 200-400 Hz. SEA cannot predict excitation at specific or narrow band frequencies. Due to the average frequency responses at a frequency band, it is incapable to predict modes or mode shapes of the system. It does not render information on local distribution vibration level within the subsystems. It is unable to give information about the spatial distribution of the field variables within each subsystem (Fahy 1994). Along with the limitations, there are various assumptions made while performing the SEA. The coupling between the subsystems is assumed to be linear and

conservative. The resonant modes in a particular frequency band are assumed to have the same amount of energy. In addition, the damping loss factor is assumed to be equal for all modes in any particular frequency band. The damping should not be too low or too high. Homogeneity of the subsystems is imperative to yield valid vibrational level calculations. Also, sound fields have to be assumed to be reverberant and diffuse (Sarradj 2004). The transmission of power from one subsystem to another subsystem is due to the existing resonant modes in the frequency band. Also the power flow within the subsystems varies proportionally to their energy level. However, SEA is simple and effective at high frequencies, particular for the cases of the present study in sound transmission loss of breakout noise from duct as discussed in Section 1.8.

1.5 Example of Simple Statistical Energy Analysis

Consider a simple example of two subsystems as shown in Figure 1.1 where there are two subsystems: Subsystem 1 and Subsystem 2. The arrow pointing towards the subsystems indicate the power received by the subsystems. While the arrows pointing away from the subsystems indicate the power lost from the subsystems. The arrows pointing within the subsystems indicate the exchange of power between the subsystems. W_1 and W_2 show the power entering the Subsystems 1 and 2, respectively, whereas W_{1d} and W_{2d} indicate the power dissipated by the Subsystems 1 and 2, respectively. W_{12} shows the power the transfer of power from Subsystem 1 to Subsystem 2, and similarly W_{21} shows the transfer of power from Subsystem 2 to Subsystem 1.
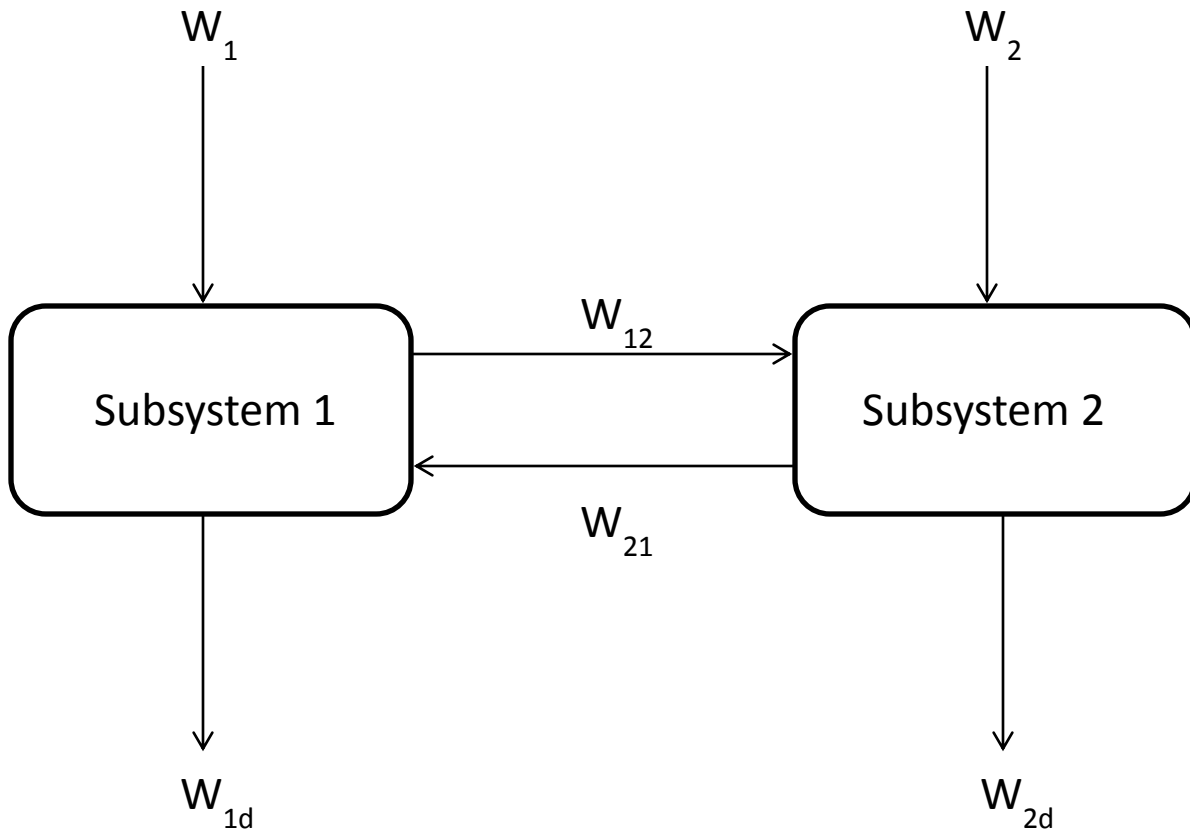
SEA model of two subsystems

Figure 1.1 - Simplistic SEA model of two subsystems in interaction.

The dissipated power at angular frequency of ω in the subsystems can be shown by the following equations,

$$W_{1d} = \omega\eta_{1d}E_1 \,, \tag{1.1}$$

and
$$W_{2d} = \omega\eta_{2d}E_2 \,, \tag{1.2}$$

where η_{1d} and η_{2d} are the damping loss factors of Subsystems 1 and 2 respectively. E_1 and E_2 are the total vibrational or acoustic energy of the modes at frequency f.

The net power transmitted between subsystems can expressed as,

$$W_{12} = \omega\eta_{12}E_1 \ , \tag{1.3}$$

and
$$W_{21} = \omega\eta_{21}E_2 \ , \tag{1.4}$$

where η_{12} and η_{21} are the coupling loss factors between the Subsystems 1 and 2.

The SEA calculation is based on energy flow equilibrium; hence the power balances for the two subsystems can be given by,

$$W_1 + W_{21} = W_{12} + W_{1d} \ , \tag{1.5}$$

and
$$W_2 + W_{12} = W_{21} + W_{2d} \ . \tag{1.6}$$

When combining the above equations, the power balance equation for the two subsystems can be expressed in matrix form as,

$$\begin{bmatrix} W_1 \\ W_2 \end{bmatrix} = \omega \begin{bmatrix} (\eta_{1d} + \eta_{12}) & -\eta_{21} \\ -\eta_{12} & (\eta_{2d} + \eta_{21}) \end{bmatrix} \begin{bmatrix} E_1 \\ E_2 \end{bmatrix} \ . \tag{1.7}$$

The generalized form of the power balance equation with *n* number of subsystems will be,

$$\begin{bmatrix} W_1 \\ W_2 \\ \vdots \\ W_n \end{bmatrix} = \omega \begin{bmatrix} \eta_1 & -\eta_{21} & \cdots & -\eta_{n1} \\ -\eta_{12} & \eta_2 & \ddots & \vdots \\ \vdots & \ddots & \ddots & \vdots \\ -\eta_{1n} & \cdots & \cdots & \eta_n \end{bmatrix} \begin{bmatrix} E_1 \\ E_2 \\ \vdots \\ E_n \end{bmatrix} \ , \tag{1.8}$$

where η_i stands for the total loss factor of the ith *system* which is the summation of the damping loss factor and the coupling loss factors and in general can be stated as (Craik 1996)

$$\eta_i = \eta_{id} + \sum_{j=1, j\neq 1}^{n} \eta_{ij} \ , \tag{1.9}$$

where n is the number of subsystems and the subscript i and j represent the identities of the subsystems.

1.6 The Need to Account for the HVAC Duct Noise.

Air ducts are responsible for providing fresh, heated or cool air for the building ensuring a pleasant climate for its inhabitants. There are, however, some inherent side effects in the ductwork that are responsible for carrying unwanted noise around the building. Noise could be generated by fans, mechanical systems or even by the air draft. The air-borne noise transmitted through the duct emerges into the building through grilles and other system outlets. This problem can be handled by lining the interior of the duct with suitable sound absorbing material or air-duct silencers. In addition to the air-borne noise from the duct outlets, sound can also be transmitted directly through the walls of the duct into the occupied space. This is called breakout noise. These distractions from both air-borne and breakout noise can cause difficulty for the occupants in terms of their ability to concentrate on their work, which in turn can affect their performance. Various attempts are being made to control this unwanted noise and present the occupants with a sound environment.

1.7 Breakout Noise in Air Duct

As discussed earlier the breakout noise in the air duct is the sound transmitted directly through the walls of the duct. It can be defined as the external radiation of acoustic power through the walls of a duct from an internal sound field. The basic assumption in defining the transmission loss, TL (ratio of incident sound power to the transmitted sound power through a partition) with

respect to the ductwork is that the sound power level inside the duct is independent of the distance along the duct. However, this assumption may not hold true because some of the acoustical energy is lost through absorption and radiation from the duct walls (Lilly, 1987).

In many models, the breakout noise prediction assumes that the sound field inside the duct is composed of one or more propagating modes (rigid duct modes or coupled structural/acoustic modes) as opposed to more or less diffuse, reverberant sound field commonly assumed to exist within building space (Cummings 1983b). The cross section geometry highly influences the breakout characteristics. The three most common cross sectional duct shapes can be seen in Figure 1.2.
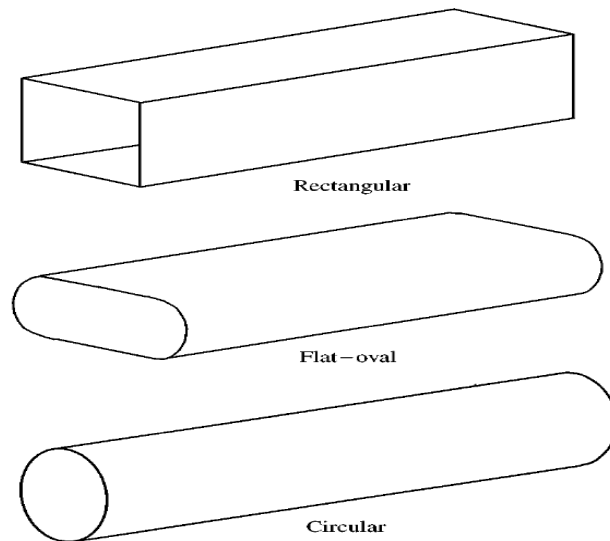
Figure 1.2 - Common cross sections of an air duct (Cummings, 2001).

There is a change in the pattern of transmission loss of the ductwork with respect to its cross sectional geometry. A rectangular duct cross section has low breakout wall transmission loss at low frequencies because of the strong structural response to the internal sound field. The circular cross-section ducts have a very high transmission loss at low frequencies. The ducts with flat oval cross sections can be expected to display the transmission loss characteristics of both, the rectangular and the circular duct cross section (Cummings, 2001).

1.8 The Need to Apply Statistical Energy Analysis on Air Duct.

There are various ways of evaluating the transmission loss for the air ducts computationally. These may include Finite Element Analysis (FEA), Boundary Element Method (BEM) etc. These methods can be employed for calculating the dynamic response at the lower order modes of a structure but when it comes to large modal density at high frequencies, these methods pose computational difficulties. The higher frequencies demand more computation and finer discretization of the geometry in order to accommodate more modes in the analysis (Shorter 2007). In addition to this, the increasing degrees of freedom poses a challenge for these methods to handle. This eventually results in longer computational times. The uncertainties of these methods highlight a need for an efficient method to understand the sound transmission at higher frequencies. The SEA is reasonably accurate at the higher frequencies as discussed earlier and the computational time is a fraction of the FEA model. As the frequency increases, the number of modes per band increases. SEA proves to be a capable tool for dealing with this issue in other applications and has been proven to produce a decreasing amount of calculation variance with the experimental measurements which will be exhibited in the succeeding sections.

1.9 The Intended Benefits of the SEA Application

In the present study, SEA is evaluated to calculate the transmission loss. The predicted data by SEA will be evaluated with the existing theoretical data (ASHRAE, 2011) for some given air duct dimensions. The existing breakout noise prediction method is listed based on the theoretical data, which is limited to the particular dimensions, wall thickness, and materials of the air duct. The SEA has the advantage of overcoming these limitations to predict the sound transmission of breakout noise for ductwork with varying material and gages (duct wall thickness) which is currently unavailable in our field.

1.10 Summary

In order to apply the Statistical Energy Analysis (SEA) for predicting the Transmission Loss (TL) of breakout noise through air duct walls, this chapter reviews the background and fundamentals of SEA. It is highlighted that SEA is effective in the prediction of dynamic behavior of a structure at high frequencies, which is the main driving force for the development of this method (SEA). The approach of SEA is chiefly focused on forming the power balance equation with the help of essential SEA parameters, for instance, damping loss factor, coupling loss factor, power (input, dissipated, transmitted) and the mode number. There are certain assumptions in the SEA methods in terms of energy distribution, nature of coupling between subsystems, homogeneity of the subsystems, etc. Moreover, there are some limitations for the SEA method with respect to its accuracy at low frequency, its capability of system mode shape predictions, etc. A simple example is stated to introduce the methodology of SEA that enables one to formulate a simple power balance equation. The need to account for the HVAC duct noise is chiefly due to the noise distraction in spaces like offices, etc. leading to an unproductive

environment. Breakout noise in air duct can be affected by the geometry of the duct (e.g. rectangular, oval, and circular); which in turn affects the transmission loss pattern for each duct geometry. SEA proposes to predict the transmission loss at high frequencies with reasonable accuracy. This method can also enable the user to predict the transmission loss of the duct irrespective of size, material and thickness with less computation time as opposed to Finite Element Analysis (FEA) and Boundary Element Method (BEM).

Chapter 2: Literature Review

There has been significant research in the field of estimating the sound transmission through air ducts by numerous researchers over the past decades. The Statistical Energy Analysis (SEA) too has gained much attention in past five decades after being developed in 1960's (Fahy, 1994). Ever since, the study of SEA has been broadened to facilitate its application in the various fields of engineering besides the aeronautical sector as initially intended. The overviews of these researches related to the SEA application and the efforts to effectively predict the sound transmission from breakout noise through air ducts have been discussed in this chapter.

2.1 Study of Sound Transmitted Through Duct Walls

Extensive theoretical and experimental investigations have been carried out by Cummings (1975a, 1975b, 1978, 1979, 1980, 1981, 1982, 1983b, 1983c, 1985, and 2001) over the years which looked into the mechanism of the transmission sound through walls of air-conditioning ducts. In dealing with sound transmission through a folded annular duct as an alternative to rectangular ducts to increase the sound transmission loss, Cummings (1975) stretched a theory of sound transmission through a 180° bend in a hard-walled rectangular duct from his previous work (1975b). Later Cummings (1978) described a one dimensional linearized analysis of fundamental mode sound generation and propagation in rigid-walled ducts with flow and axial temperature variation. The study intended to investigate the situation where both the mean axial flow and temperature gradients were present inside the duct. Cummings (1979) has also dealt with the attenuation of lined plenum chambers in duct systems and proposed a design procedure

for plena. In a study investigating the use of line source theoretical models to predict the low frequency radiation from the walls of the duct, Cummings (1980) was successful in predicting both the far field directivity of radiation at discrete frequencies and total radiated power. The theoretical predictions showed a good agreement with the experimental results. In an attempt to address the prediction of low frequency acoustic transmission through the walls of the rectangular ducts, Cummings (1981) proposed the use of design charts as a substitute for lengthy calculations that could have been time consuming to program on a computer.

Cummings (1982) also investigated the prediction of pressure fields for one- and two-dimensional numerical models of non-uniform lined duct with experiments. The method validated one-dimensional model for frequencies below the cut-on frequency of the first transverse mode. The two-dimensional models yielded reasonable results at frequencies below and above the cut-on frequency of the first transverse modes though it was highly sensitive to multidimensional acoustic fields. Cummings (1983b) discussed the idea of the asymptotic solutions for high-frequency acoustic transmission through the walls of the rectangular ducts. Cummings (1983c) had also authenticated a closed form solution of the structural wave equation governing the motion of the duct wall. The solution is used to predict the response of the walls to the internal pressure field and the transmission of internally propagated higher order acoustic modes through the duct walls. While investigating internally propagated sound through the walls of air conditioning ducts with different cross sectional geometry, Cummings (1985) devised a prediction method for the insertion loss of the external acoustic lagging for rectangular duct, circular and flat-oval cross section duct. The predictions have been compared with experimental results. This study also referred to an earlier experimental investigation by Guthrie (1979) in which the low-frequency internal/external sound transmission through the walls of rectangular

and flat-oval ductwork had been studied. There was another method for computing the total radiated sound power level from breakout noise in HVAC ductwork by Lilly (1987). The study presented a simple analytical method for computing breakout noise based on the idea of computing total radiated sound by the incorporating the acoustic intensity outside the duct over its entire surface area. It made an emphasis on the fact that the total power radiated from the duct was not just dependent on the inlet power and transmission loss but also on the total exposed duct surface area and the attenuation constant. However, the study was more suited for spiral round duct. Cummings (2001) also addressed the issue of acoustic breakout and breakin sound through duct walls by making an effort to identify the main physical processes involved. The study also commented on the future area of research in terms of clarifying the relative roles of the structural and acoustic types of coupled modes in sound transmission, ways of modeling complex systems and need for developing pure numerical methods to yield accurate prediction results.

2.2 Study on Statistical Energy Analysis

There have been multiple reviews in the past of statistical energy analysis (SEA) since its development. Woodhouse (1981a) had investigated the use of SEA for vibration analysis. The study discussed the possible methods of measuring the SEA parameters in a given problem and enabled the user to decide whether SEA was indeed suitable for that given problem. It also guided the users with SEA's application especially helping them to divide subsystems. Woodhouse (1981b) had also discussed SEA applications in structural vibration using Rayleigh's classical approach in order to study systems with a finite number of degrees of freedom. Some

modifications had been suggested to strategize SEA modeling based on the type of coupling involved.

Heckl and Lewit (1994) applied statistical energy analysis to experimentally and numerically quantify sound and vibration transmission path of three plates. They investigated the energy flow and the coupling properties in order to find the paths responsible for sound transmission in complex structure. It eventually assisted in optimizing the measure for noise control. Heckl and Lewit (1994) further proposed to determine SEA temperature by stating that energy per mode and coupling loss factor are analogies of temperature and heat conduction coefficient, respectively. These analogies assist in evaluating the direction of sound and vibration transmission. Moreover, an analysis on the nature (strong and weak) of couplings of subsystems was also made based on the temperature difference (Heckl and Lewit, 1994). Related to SEA temperatures, there has also been a study on the use of entropy balance as opposed to energy balance in dealing with SEA problem (Le Bot et al., 2011). The study of entropy balance as an alternative technique was on the backdrop of SEA origin from statistical mechanics and thermodynamics. The study further stretched beyond the use of SEA which for a long time was limited to the application of the first principle of thermodynamics (energy balance) by introducing the idea of having an entropy balance as a substitute to the energy balance.

A critical overview of SEA by Fahy (1994) discussed the principles for the use of probabilistic energetic models of SEA for prediction of high-frequency vibration. It also stated the strength and weaknesses of SEA. It illustrated the different approaches to SEA viz: (1) modal approach, (2) wave approach, (3) mobility approach, (4) modal energy and (5) wave intensity, etc. It discussed the contemporary deficiencies in SEA approaches. Some of the deficiencies are: (1) though being a probabilistic approach, there is no proven procedure for making the estimates of

confidence in the predicted results; (2) the inability of SEA to deal with the narrow band and tonal excitation without auxiliary statistical data for the energy response functions for directly or indirectly driven subsystems of various generic forms; and (3) providing no information about the spatial distribution of the field variables within each subsystem, etc. SEA's conspicuous success in dealing with vibro-acoustic problems involving the interaction of broadband sound fields in air with structures has been discussed. Fahy (1994) also suggested further research in terms of handling highly non-uniform structural components, study of spatial distribution statistics of response variables, developing a generalized method for predicting indirect power transfer coefficients, etc.

There have been some publications tackling complex problems by SEA involving complex geometry. Lyon and DeJong (1995) provided exhaustive testing of theory and application of SEA in acoustics and vibration. In addition to predicting noise and vibration transmission, they also explore the impact of SEA in computer power and resources.

Burroughs et al. (1997) had also reviewed the basic concepts of SEA. The study developed a power balance equation for coupled simple oscillators with resonant modes. Assumptions in SEA had been discussed with regard to the frequencies of resonance for each subsystem to be uniformly distributed in frequency within each of the frequency bands used in the analysis. Therefore, assuming energy resides only in resonant modes, the total energy in each subsystem is the sum of the energies in the modes. The energy is thus assumed to be equally distributed among the modes in each subsystem and frequency band. The study also outlined the methods for obtaining the parameters required to predict the energy distribution within a system using power balance equations.

Sarradj (2004) had discussed the basic ideas behind the method for the treatment of vibro-acoustic problems, which are based on energy variables like energy density, power, etc. as opposed to quantities such as force and displacement. The theory and application of SEA regarded as the most popular method was also explained. Besides introducing SEA in the traditional format, Sarradj (2004) has addressed the limitations of SEA in terms of weak couplings, extent of damping, homogeneity of the subsystems, etc. To overcome some of these limitations, he proposed methods such as: (1) wave intensity analysis to avoid the diffuse field assumption in the subsystem, (2) energy finite element method to deal with heat conduction, (3) smooth energy model or high frequency boundary element method to formulate a boundary integral using energy variables, (4) energetic mean mobility approach that accommodates heterogeneous structures, (5) complex envelope distribution analysis with a cepstrum calculated from wavenumber spectrum in contrast to the frequency spectrum, and finally (6) hybrid methods to incorporate prominent modal behavior of components into SEA-like models.

The research in the field of SEA had been stretched further (Le Bolt and Cotoni, 2010) concerned with its validity which can be defined in terms of four criteria: (1) mode count, (2) modal overlap, (3) attenuation factor, and (4) coupling strength. It suggested that the mode count (i.e. number of modes per unit frequency) and the modal overlap should be high. Moreover, the normalized attenuation factor (i.e. sound absorption factor) and coupling strength (i.e. strength of force exerted in an interaction) must be low. The idea of applying the dimensional analysis to exhibit the space of dimensionless parameters for validation was conducted on a vibrating system of rectangular plates. The diagrams for SEA validity were introduced and discussed. In-order to illustrate the usefulness of validity diagrams, a numerical simulation was presented on a pair of coupled rectangular plates. It also commented that the four criteria discussed earlier for

validity domain of SEA were not the only criteria to entirely define the validity domain of SEA. This was because of some other assumptions, such as nature of excitation and the problem of variance in SEA were not been discussed in the study.

A study was also been carried out to apply the graph theory for noise and vibration control using SEA (Guasch and Cortes, 2009). It established a combined path-algebras and standard linear matrix algebra to derive several transmission path results in a generalized mathematical framework. SEA graphs have been developed based on the SEA schematic models with nodes representing subsystems and edges existing between subsystems having non-null coupling loss factors. In addition, a scheme that makes use of graph cut algorithms (used to locate minimum cut in SEA graph that separates a source subsystem from the receiver subsystem) had been introduced to reduce the energy at the target subsystem by modifying as fewer system loss factors as possible; thus enabling a beneficial strategy from an engineering perspective.

2.3 SEA in Noise Control Applications

While discussing the insertion loss of a closed space, for instance air duct, enclosure, room etc., theoretical models based on Statistical Energy Analysis (SEA) for insertion loss of an acoustic enclosure had been established by Ming and Pan (2004). The non-resonant transmission (i.e. trace wave (moving along the surface of the enclosure wall) generated by the incident acoustic excitation field) and the interaction between enclosure walls were included in the models. It was demonstrated that the insertion loss of an acoustic enclosure was chiefly governed by the non-resonant modes at the intermediate frequencies because of a very low radiation capacity at the resonant modes. This experimental study was carried out using two types of acoustical

enclosures: a rectangular box enclosure and an enclosure with fibrous glass composite panels. The measured results were compared with the predicted values.

To deal with the issue of non-resonant transmission, an earlier study had addressed the inability of conventional SEA to predict the non-resonant response of the structure (Ranji and Nair, 2001). The study presented a modified SEA formulation in which the non-resonant responses could be estimated. The formulation was similar to the conventional SEA modeling for resonant response but different expressions for the coupling loss factors was proposed. Two reverberant rooms separated by a panel were set as example in their study.

Sgard et al. (2010) predicted the acoustical performance of enclosure using the hybrid statistical energy analysis. A general and simple model was proposed for predicting the acoustic performance of a large free-standing enclosure. The model was able to handle the complexity of the enclosure configuration at a large frequency range. The hybrid method combined the SEA for the sound transmission across the various elements of the enclosure and the image sources method for the sound field inside the enclosure. The approach claimed to have the features to offer more flexibility to calculate the coupling loss factors for various sound absorbing materials. The study affirmed the use of image source technique as an adept description of internal sound field to account for the location of the acoustic source in the enclosure. Hence it proposed the combination of the coherent image source method and SEA as a reliable tool to predict the acoustics at low frequencies.

A hybrid method had also been suggested earlier by Langley (1999) for dynamic analysis of complex systems. The method was based on partitioning the degrees of freedom into "global" set and "local" set. The method was found to yield good results for simple systems. It involved the

unification of a number of different analytical methods, for instance, the finite element method, the statistical energy analysis (SEA), fuzzy structure theory and the Belyaev ''smooth function'' approach (Belyaev, 1993).

Lie et al. (2012) discussed about the discrepancies between the SEA prediction and measured results especially at the low and intermediate frequencies. In the study, the sources of discrepancy (e.g. incompatible boundary conditions and measurement point distribution) were identified by an investigation of the limitations of SEA for energy transfer in the entire frequency range and by the effect of structure-structure coupling and acoustic-structure coupling on prediction of noise reduction. The predicted structural response and the noise reduction of an acoustical enclosure (of a specified dimension and material properties) were compared with the experimental results for validation.

Most theories of SEA in past few decades could only accurately predict the transmission loss for right-angled wall junctions in buildings, but non right-angled junctions in the buildings has not been addressed. This information is of extreme significance in modern high-rise buildings because of complex structure. The study by Tang (2005) measured the total loss factors and vibrational power transmission losses in existing buildings having non right-angled wall junctions. The dependence of vibration power transmission was also discussed.

2.4 Study on Some Essential Parameters of SEA

There has been a comprehensive research to deal with the radiation efficiency that relates to the radiated power with spatially averaged vibration of the system. In SEA, it is an instrument in estimating the coupling loss factor between the air and solid structures. A considerable study had

been conducted in investigating the radiation efficiency of plates using the modal summation approach (Xie et al., 2005). The study confirmed the vital radiation efficiency equations from Ver and Homer (1971) in prediction of the radiation efficiency of the plates.

For determining the non-resonant transmission, an essential parameter is the transmission coefficient which gives ratio of the total power transmitted through a system to the total power incident on it. The transmission coefficient is useful to calculate the non resonant coupling loss factor. Beranek and Ver (1992) established a formulation of sound reduction index for various cases that they are widely used in SEA applications. In an earlier study, Langley (1990) had discussed a calculation of the wave transmission coefficients of structural joints. The study considered a simple plate/beam junction consisting of arbitrary number of plates either coupled through a beam or directly coupled through a line.

Sometimes when a structure is modified, it demands re-analysis for yielding the desired results. This issue had been studied and addressed by Thite (2010). The study suggested that Apparent Coupling Loss Factors (ACLF) (i.e. coupling loss factor calculated for modified analysis) could be estimated in the manner similar to that in a conventional SEA. The calculation of ACLF could enable the analysis of a modified structure without re-analysis as in conventional SEA thereby claiming this method to be computationally efficient.

Considering vibrational energy distribution between two coupled plates, a study in determination of the plate loss factors (or so called internal loss factors) and coupling loss factors by power injection method (Bies, 1980) had been carried out in order to determine the loss factors by the inversion of linear power balance equations. It was suggested that the modal statistical independence (i.e. independent evaluation of quantities such as modal densities of the

subsytems, etc.) could be adequately approximated by the means of injecting power at three or more points in the chosen system. The loss factors obtained by this method were in good agreement with the steady state determinations of the same quantities.

An attempt made on a scaling procedure intended to reduce the computational costs associated with a deterministic approach in wavelength simulation (Rosa, 2010). The results obtained from standard techniques as Classical Modal Analysis (CMA) and Statistical Energy Analysis (SEA) were compared with an innovative approach called Asymptotic Scaled Modal Analysis (ASMA). It inferred that ASMA was not as effective as SEA, but it could however be served as a useful tool to SEA in structural configurations where analytical solutions were not available.

An attempt had been made to present a new and efficient method to calculate point mobilities from subcomponents of a full structure (Ragnarsson et al., 2010). Earlier subcomponent modeling had been used to obtain information on dynamic behavior of complex assembly structures using smaller and more efficient models. Point mobility calculations at the subcomponent level are employed to obtain more precise parameters of SEA models. Since complete system analysis is often computationally expensive, so only the individual subcomponents are selected and analyzed. Though this procedure saves computational effort, it also results in significant loss of accuracy. This error can be attributed to the approximation used in defining the boundary conditions. To address this issue, by taking a cue from an earlier work which demonstrated a certain level of accuracy in achieving the boundary condition of a structure by describing the interface dynamics by a combination of dynamic waves; the authors in this study developed the method further to present a more robust and an efficient wave extraction procedure.

2.5 Application of SEA in Other Fields.

 The SEA has broadened its gamut of applications. It has also been applied successfully in many other areas such as ships, aircrafts, car etc. An acoustic research on electric motor quantified the transmission of vibrations from stator yoke to motor frame (Delaere et al, 1999) in the stator yoke and in the coils of the electric motor. SEA proved to be a valuable tool in handling the composed systems with high modal density (for high frequencies) for the noise research of these electric machines. SEA has also been used to study the subdivision of a volume of air in a vehicle enclosure into SEA subsystems (Fahy, 2004). The study simply tried to suggest that the subdivision of air space into SEA subsystems was acceptable in cases where the sound field may be reasonably considered to be approximate the ideal diffuse field.

Burkett (2007) dealt with the prediction of interior noise levels in a cabin of a freightliner where SEA was used to simulate noise levels. The impacts of different types of absorptive materials, main paths and flaking paths were studied. The engineers focused on the control of flanking paths which resulted in significant reduction of noise as compared to the earlier designs of the cabin. It was claimed to be the quietest cabin in North America.

2.6 ASHRAE References

To predict the sound transmission loss through air duct, the theoretical results in ASHRAE Handbook: HVAC Application (2011) based on Lilly's theory (1987) has been widely used for various cross-sectional duct geometry at octave band frequencies.

$$TL_{out} = L_{w(in)} - L_{w(out)} - 10 \log\left(\frac{S^*}{A}\right) \tag{2.1}$$

where TL_{out} is the transmission loss of breakout noise, $L_{w(in)}$ is the sound power level inside the air duct, $L_{w(out)}$ is the sound power level radiated out through the surface duct walls, S^* is the effective surface area and A is the cross sectional area of the duct.

$$S^* = 2L^*(larger\ c/s + smaller\ c/s)\ ,$$ (2.2)

L^* is the effective length of the duct given as,

$$L^* = \frac{\gamma_1^{\ L} - 1}{\ln(\gamma_1)}$$ (2.3)

where,

$$\gamma_1 = 10^{-\frac{\alpha}{10}}$$ (2.4)

α is the duct attenuation factor.

The ducts used in the study are of the material "galvanized steel" of various gages (i.e. duct thickness). The confining feature of the listed TL data in ASHRAE is that it is limited to certain dimensions and gages only. The duct material limits itself only to galvanized steel. This in turn limits the estimation of TL to only certain duct configurations.

The thickness of the sheet metal for galvanized steel quantified by the different gages are cited from ASHRAE Handbook: Systems and Equipment (2012).

2.7 Summary

There has been substantive research in the field sound transmission for breakout noise through air ducts. These researches have suggested improved ways of predicting results, but it still poses

a challenge for computation. The SEA over the years has emerged to be a better alternative and computation efficiency to conventional deterministic methods to predict the behavior of the structure at relatively high frequencies. Researches in improving the level of prediction of SEA have been undertaken over the period of time. Methods of validating SEA also have been successfully carried out. The various parameters involved in SEA approach are being improvised which enable the analysis to get more accurate results thus reducing the minimal existing discrepancies. The SEA application has also gained popularity in various sectors other than civil structures like appliances, motor industry, etc. Hence, by studying the practical background of SEA, an attempt can be made in extending its validity to problems involving the prediction of the sound transmission for air ducts, which have not been addressed so far.

Chapter 3: Methodology

3.1 Duct Model

To evaluate the Statistical Energy Analysis (SEA) in prediction of the Transmission Loss (TL) of breakout noise through the air duct walls, a random configuration of the duct for listed theoretical data in the ASHRAE Handbook: HVAC Applications (2011) is selected in the present study. The predicted transmission losses are then compared with the theoretical data (ASHRAE, 2011) at octave band frequencies as listed.

The model chosen for numerical analysis is an unlined rectangular duct of cross section 0.305 m x 0. 610 m, the length being 6.1 m. The rectangular duct model consists of two pairs of duct wall panels in dimensions of 0.305 m x 6.1 m and 0.610 m x 6.1 m, respectively. It is open at both ends of the cross sections 0.305 m x 0.610 m as shown in the Figure 3.1. The material of the duct wall panels are composed of 24 gage galvanized steel having the modulus of elasticity E = 210 GPa, Poisson's ratio μ = 0.3125, and density ρ = 7800 kg/m^3. The thickness of the duct wall panel (24 gage), h, is 0.7 x 10^{-3} m (ASHRAE, 2012).

While applying the SEA, the model is divided into individual subsystems with an assumption of diffuse energy in each subsystem. The air duct is divided in six subsystems: four duct walls, the internal air cavity and the external air space. The numbering of subsystems is established in the direction of flow of energy from the internal air cavity into the walls of the air duct and transmitted to the external space as shown in Figure 3.2. The internal air cavity with the dimension 0.610 m x 0.305 m x 6.1 m is considered as Subsystem 1. The two duct-wall panels (plates) with dimensions 0.305 m x 6.1 m x 0.7 mm are considered to be Subsystem 2 and Subsystem 4, which are denoted by plate i and k, respectively. The other two duct-wall panels

(plates) with dimensions 0.610 m x 6.1 m x 0.7 mm are considered to be Subsystem 3 and Subsystem 5, which are denoted by plates *j* and *l*, respectively. The external air space is considered to be Subsystem 6. The sound transmission loss is evaluated by the difference between the acoustic energies inside the internal air cavity and external air space.
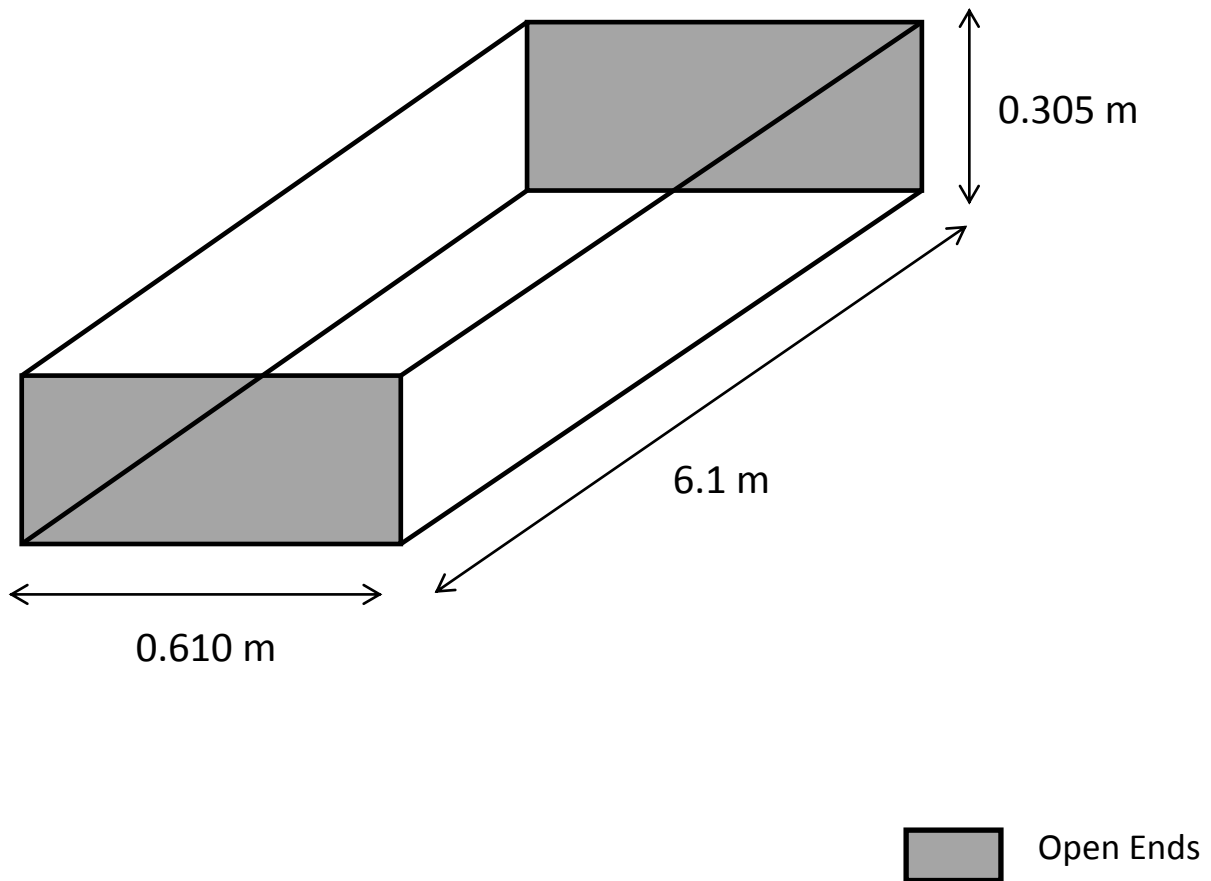
Figure 3.1 - Simple geometry of the duct model.

W_{26}

W_{23}

Subsystem 2
(Plate i)

Subsystem 3
(Plate j)

W_{32}

W_{36}

W_{12}

W_{21}

W_{13}

W_{31}

W_{52} W_{25}

Subsystem 1
(Internal Air Cavity)

W_{43} W_{34}

W_{51}

W_{14}

W_{15}

W_{41}

W_{54}

Subsystem 5
(Plate l)

Subsystem 4
(Plate k)

W_{45}

W_{56}

W_{46}

Subsystem 6
(External Space)
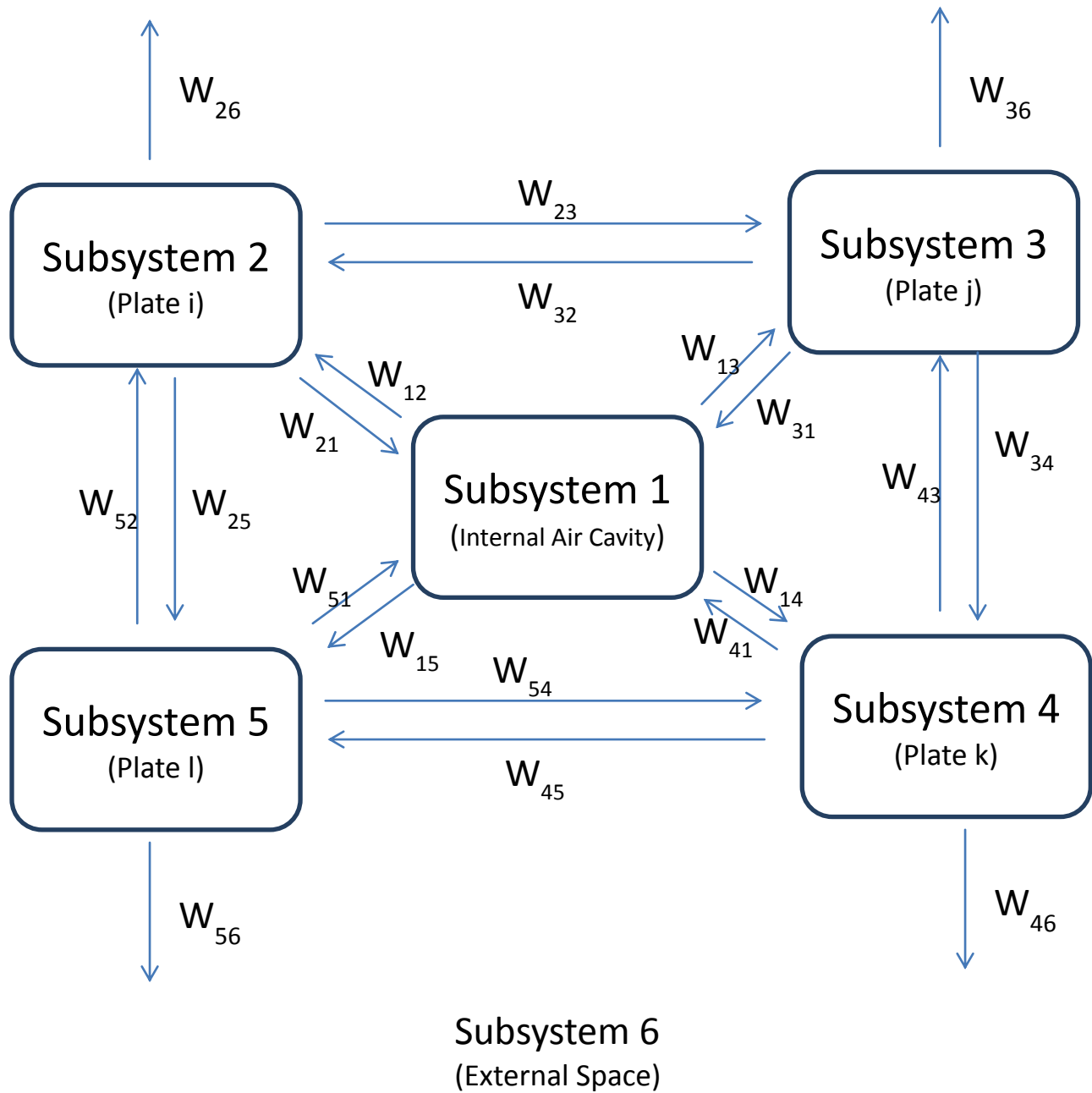
Figure 3.2 - Schematic representation of exchange of power within subsystems.

Figure 3.2 shows the schematic representation of the SEA model and the interaction of the subsystems within themselves. The arrows pointing inwards and outwards of a system represent the energy received into and energy lost from the corresponding subsystem, respectively. The arrows pointing between the subsystems show the paths by which energy is transmitted from one

subsystem to another. Therefore, W_{12} indicates the energy flow from Subsystem 1 to Subsystem 2. Likewise, W_{21} indicates the energy flow from Subsystem 2 to Subsystem 1.

It is observed that Subsystem 1, which is the internal air cavity, transmits energy to and receives energy from the four other subsystems (i.e. Subsystems 2, 3, 4 and 5). As mentioned earlier (in Section 1.2) regarding the exchange of energy between the subsystems, it is observed that some subsystems do not interact (i.e. energy exchange) with each other. As seen in Figure 3.2, there is no exchange of energy between Subsystems 2 and Subsystem 4, and also, between Subsystem 3 and Subsystem 5. This is because the subsystems (plates in our model) are not directly connected, hence the effect of any coupling between them can be neglected. It is further observed that Subsystems 2, 3, 4 and 5 (i.e. all duct wall panels) transfer energy to Subsystem 6 which is an infinitely large external space. Due to this large external space, there is negligible energy return from Subsystem 6 to Subsystem 2, 3, 4 and 5. However, there will be a non-resonant path discussed in Section 3.10, which could transfer energy from Subsystem 6 to Subsystem 1 and vice versa.

The noise source inside the duct cavity generates an internal sound field, which in turn excites vibration of duct walls. The vibrating walls will then radiate noise into the area outside the duct (external space). The duct walls (i.e. the plates in the model) are assumed to be flexible, homogeneous, isotropic, thin and of uniform thickness. Due to the thin structures of the duct walls, the effect of shear stress deformation and rotational inertia are negligible. Only bending waves are considered in the analysis. The fundamental resonance frequency of the plates is smaller than the lowest natural frequency of the enclosed volume. The first three lowest axial resonance frequencies for the plates with dimension 0.305 m x 6.1 m are 0.046 Hz, 18.66 Hz and 18.71 Hz and for plates with dimension 0.610 m x 6.1 m are 0.046 Hz, 4.67 Hz and 4.71 Hz,

respectively. The first three lowest axial resonance frequencies for the cavity (enclosed volume) are 281.15 Hz, 562.3 Hz and 628.67 Hz respectively.

3.2 Critical Frequency and the First Resonant Frequency of the Duct Wall Panels

The frequency at which the projected airborne wavelength coincides with the solid-borne wavelength at a certain angle of incidence, the frequency can be termed as a critical frequency. The critical frequency is an instrument in determining the radiation coefficient (discussed in Section 3.5) at the driving frequency from the wall panels in SEA. It is also useful in studying the response of the system for resonant and non-resonant parts (discussed later in Section 3.10) because generally the nature of these responses change when close to, and over the critical frequency (Craik, 1996). The critical frequency is given as

$$f_c = \sqrt{\frac{3c^4\rho_s(1-\mu^2)}{\pi^2 E h^3}} \quad , \tag{3.1}$$

where c denotes the speed of sound in air and ρ_s is the surface density of the duct. The Poisson's ratio of the duct material is given by μ and the modulus of elasticity of the duct material is represented by E, while h is the thickness of the duct.

The first vibration resonance frequency of the duct wall can be calculated as follows (SS-EN12354-1, 2000),

$$f_{11} = \frac{c^2}{4f_c}\left(\frac{1}{l_1^2} + \frac{1}{l_2^2}\right) \quad , \tag{3.2}$$

where l_1 and l_2 are the dimensions of the duct wall panel.

3.3 Internal Loss Factor of the Enclosed Air Volume Inside the Duct

The internal loss factor is the result of energy losses caused due to internal losses (i.e. transformation of heat) or radiation. It thus amounts to the fraction of energy lost as heat in one radian cycle of excitation. The Subsystem 1 comprising of the enclosed air volume has a dominance of viscous loss and thermal loss at the walls. The internal loss factor can be calculated by (Eichler, 1965),

$$\eta_{11} = \frac{S_a c \gamma}{4 \omega V} \quad , \tag{3.3}$$

where the total internal surface area of the cavity is represented by S_a, while ω denotes the angular frequency (i.e. $2 \pi f$). The volume of air cavity inside the duct is V. The acoustic absorption coefficient of the wall surface is represented by γ. For our case, no absorption material is present inside the duct. For the case at room temperature, the acoustic absorption coefficient can be set by (Kutruff, 1979)

$$\gamma = 1.8 \times 10^{-4} \sqrt{f} \quad . \tag{3.4}$$

3.4 Dissipation Loss Factors of the Duct Wall Panels (or called Plates)

The dissipation loss factor is the measure of the loss-rate of energy of a mode of oscillation in a dissipative system. In the case below, the dissipation loss factor is evaluated by summing the structural damping and radiation loss factor. The structural damping dominates the dissipation loss factor at octave bands below the critical frequency, while the radiation loss dominates at frequencies above the critical frequency (Ming and Pan, 2004). The dissipation loss factors of a plate can be found by,

$$\eta_s = \frac{0.7}{f^{0.9}}. \tag{3.5}$$

3.5 Radiation Coefficients for the Duct Walls Panels (or called Plates)

Sound radiation from a rectangular plate to fluid is of paramount importance for sound transmission. The radiation coefficient is an essential parameter in evaluating the coupling loss factor between the plate and the fluid (Section 3.6). There can be any medium surrounding the plate, such as air, water or any other fluid or gas. The interaction between the plates and its surrounding medium can be described by the radiation coefficient. The radiation coefficient is useful in calculating the coupling loss factor (Section 3.6) from the plate to the cavity in our study. There are two frequencies that are vital for the calculation of the radiation factors: (1) the frequency of the first mode of the plate and (2) the critical frequency of the plate.

Ver (1971) defines radiation efficiency for all possible cases of the radiation factors σ. For the first case, where the driving frequency is less than the first resonance frequency f_{11}, i.e. $f < f_{11}$

$$\sigma = \frac{4S_l}{c^2} f^2 . \tag{3.6}$$

For $f_{11} < f < f_e$,

$$\sigma = \frac{4\pi^2}{c^2 S_l} \frac{B}{m''} \quad . \tag{3.7}$$

For $f_e < f < f_c$,

$$\sigma = \frac{P_l c}{4\pi^2 S_l f_c} \times \frac{(1-\beta^2)\ln\left(\frac{1+\beta}{1-\beta}\right)+2\beta}{(1-\beta^2)^{\frac{3}{2}}} \quad . \tag{3.8}$$

For $f = f_c$,

$$\sigma = 0.45\sqrt{\frac{P_l f_c}{c}} \quad . \tag{3.9}$$

For $f > f_c$,

$$\sigma = \left(1 - \frac{f_c}{f}\right)^{-\frac{1}{2}} \quad . \tag{3.10}$$

For the above equations, $f_e = 3c/P_l$; the speed of sound is denoted by c; P_l is the perimeter the plate; S_l is the area of the plate; B is the bending stiffness; m'' is mass per unit area of the plate; and

$$\beta = \sqrt{\frac{f}{f_c}} \quad . \tag{3.11}$$

3.6 Coupling Loss Factor

The coupling loss factor is an essential parameter in SEA. It is associated with the energy transmitted from one subsystem to another. The formulation of coupling loss factors depends on the type of junctions and the properties of the subsystems. It can be best defined as the fraction of energy transmitted from one subsystem to another in one radian cycle. Two types of coupling

loss factors will be discussed in this section comprising of coupling loss factor from a plate to an internal air space and coupling loss factor between two plates.

The coupling loss factor from a plate to the internal air volume can be divided into two cases (Price and Crocker, 1970). (1) If the evaluated frequency is less than the critical frequency (i.e. $f < f_c$), the coupling loss factor can be found by,

$$\eta_{ia} = \frac{2\rho_0 c \sigma_i}{\omega \rho_{s_i}} \quad , \tag{3.12}$$

where η_{ia} is the coupling loss factor between the plate i and the air cavity a. ρ_0 is the density of air. σ_i is the radiation coefficient of plate i and ρ_{s_i} is the surface mass density of plate i. If the forcing frequency is greater than or equal to the critical frequency (i.e. $f \geq f_c$,), the coupling loss factor is given by,

$$\eta_{ia} = \frac{\rho_0 c \sigma_i}{\omega \rho_{s_i}} \quad . \tag{3.13}$$

The coupling loss factors from the internal air volume and the plate can also be obtained from the consistency relationship that will be discussed later in Section 3.8.

The coupling loss factor between the plates can be determined by the method shown in Bies (1980). Since the plates have the same material properties and same thickness, the density and longitudinal wave speed of the plates are the same and the formulation of the coupling loss factor between plates can be simplified as,

$$\eta_{ij} = \frac{0.2068 c_B L_{ij}}{\omega S_i} \quad , \tag{3.14}$$

where c_B is the bending wave speed of the wall. Bending wave for the duct wall panel is responsible for sound radiation through the duct wall as it deforms the structure transversely as vibration propagates. The L_{ij} represents the coupling length or the length of the junction between the plates. In the case above, it represents the junction length between plate i and plate j. S_i denotes the surface area of the duct wall panel i.

The bending wave speed of the plate can be given as follows, (Craik, 1996)

$$c_B = \left(\frac{4\pi^2 f^2 B}{\rho_s}\right)^{\frac{1}{4}} \quad , \tag{3.15}$$

where ρ_s is the surface mass density of the plate and B is the bending stiffness which can be estimated based on the elastic modulus and the moment of inertia of the plate as,

$$B = \frac{Eh^3}{12(1-\mu^2)} \quad . \tag{3.16}$$

3.7 Modal Density

In SEA, acoustic and vibration modes play a vital part. They occur when the multiple of half wavelengths and the dimensions of the subsystem coincide. This results in the increase in wave amplitude between the waves travelling in the subsystem due to constructive interference. Modes within the subsystem are responsible for receiving, storing and transferring the energy. The modal density presents the number of modes per unit frequency. It is essential in calculating the unknown coupling loss factor of a particular subsystem by the consistency relationship. If the coupling loss factors in both directions between all the subsystems in the model are known, then evaluating the modal density may not be a requisite.

In the present study, the modal density of the enclosed air volume can be given as, (Kutruff, 1979)

$$n_a = \frac{4\pi f^2 V}{c^3} + \frac{\pi f S}{2c^2} + \frac{P}{8c} \quad , \tag{3.17}$$

where V represents the internal enclosed air volume. S is the total surface area of the plates. P denotes the total length of the edges. Compatible with the geometry of the plates, the modal density of the plate i is defined by (Kutruff, 1979),

$$n_i = \frac{\sqrt{3}S_i}{c_L h} \quad , \tag{3.18}$$

where c_L represents the longitudinal wave speed on the plate. S_i is the total surface area of the plate i. The longitudinal waves play an important part in the sound transmission, as they are dominant in the fluid medium that is air in the present study. The longitudinal wave speed can be evaluated as follows (Craik, 1996),

$$c_L = \sqrt{\frac{E}{\rho(1-\mu^2)}} \quad . \tag{3.19}$$

Similarly, the modal densities for plate j, k and l can also be estimated as,

$$n_j = \frac{\sqrt{3}S_j}{c_L h}, \qquad n_k = \frac{\sqrt{3}S_k}{c_L h}, \qquad n_l = \frac{\sqrt{3}S_l}{c_L h}. \tag{3.20}$$

3.8 Consistency Relationship

The modal density is useful in finding the coupling loss factor of an unknown subsystem. This can be achieved by applying the consistency relationship. This relationship is established

between two subsystems with their modal densities and corresponding coupling loss factors. The application of consistency relationship can lower the computational time and memory usage. As in the case below, the coupling loss factors between plate i and plate j can be related by their respective modal densities (Craik, 1996),

$$\eta_{ij}n_i = \eta_{ji}n_j. \tag{3.21}$$

Similarly the coupling loss factors for all the connected subsystem can be found with the consistency relationship and their modal densities using Equation (3.21).

3.9 Evaluating the Total Loss Factors

The total loss factor gives the measure of the total energy lost in each radian cycle due to all mechanisms of transmission. The total loss factor amounts to the sum of all coupling loss factors from the one subsystem to all the other connected subsystems and the internal loss factor. It can also be described as system's damping (Craik,1996) and can be expressed as,

$$\eta_i = \sum_{j=1,j\neq i}^{t} \eta_{ij} + \eta_s \ , \tag{3.22}$$

where t represents the number of subsystems.

3.10 Non-Resonant Coupling Loss Factor

The SEA is chiefly focused on calculating the responses for resonant transmission between subsystems. The basic assumption of the SEA model is that the energy in each subsystem is contained in the resonant modes so that the energy is proportional to the damping. However, the response of an element is sometimes not proportional to the damping. In this case, the excited

behavior is non-resonant. For coupling between two subsystems separated by a plate or a wall, when there is a transmission through the plate at frequency below the resonant frequency of the plate, the transmission can be termed as non-resonant transmission. The non-resonant coupling loss factor between the internal air cavity and the external space can be given as (Craik, 1996),

$$\eta_{at} = \frac{13.7 S_t \tau}{fV} \ , \tag{3.23}$$

where S_t is the total surface area of the plates and V is the internal air volume. The transmission coefficient is represented by τ. In general, the transmission coefficient can be calculated by knowing the sound reduction index (Craik, 1996),

$$R = 10 \log \left(\frac{1}{\tau} \right) \ , \tag{3.24}$$

where R represents the sound reduction index. This non-resonant sound reduction index can be calculated shown by Beranek and Ver (1992),

$$R = 20 \log (f \rho_s) - 42. \tag{3.25}$$

3.11 Evaluating the Sound Power Levels

The power flow between two subsystems is the product of energy, angular frequency and the coupling loss factor. The power flow from one subsystem to another, i to j, can be represented as,

$$W_{ij} = E_i \omega \eta_{ij} \ , \tag{3.26}$$

where E_i represents energy in subsystem i.

The mass of the plates m, play an important role in order to evaluate the average vibrational velocity v, which is important in estimating the sound power radiate by the resonant modes of the duct wall and can be expressed as (Norton, 1999)

$$m = \rho V_p \quad , \tag{3.27}$$

where V_p is the volume of the plate.

The average vibration velocity can be then calculated by (Norton, 1999),

$$v = \sqrt{\frac{E}{m}} \quad , \tag{3.28}$$

where E is the average vibration energy of the plate. The sound power of the internal sound field can be computed by,

$$W_e = \omega \eta_a E_a. \tag{3.29}$$

The resonant sound power radiated by each wall of the air duct can be expressed as (Norton, 1999),

$$W_r = \rho_0 c \sigma_i S_i v_i^2 \quad . \tag{3.30}$$

where $\sigma_i, S_i \ and \ v_i^2$ are the radiation coefficient, surface area and the vibrational velocity of plate i respectively.

The non-resonant sound power radiated by the non-resonant modes of the duct wall panel can be represented by,

$$W_n = \tau W_e \quad . \tag{3.31}$$

The total sound power radiated from the enclosure can be shown as,

$$W_{total} = \sum W_r + W_n \ . \tag{3.32}$$

The general power balance equation for *t* subsystems can be formed as,

$$\omega \eta_i E_i - \omega \sum_{j=1, j \neq i}^{a} \eta_{ji} E_j = 0 \ , \qquad i = 1, 2, \dots t \tag{3.33a}$$

$$\omega \eta_a E_a - \omega \sum_{j=1}^{t} \eta_{ja} E_j = W_e. \tag{3.33}$$

Assuming the power input as 1W, Equation 3.33 can be expressed in matrix form as,

$$\begin{bmatrix} \eta_1 & -\eta_{21} & -\eta_{31} & -\eta_{41} & -\eta_{51} \\ -\eta_{12} & \eta_2 & -\eta_{32} & 0 & -\eta_{52} \\ -\eta_{13} & -\eta_{23} & \eta_3 & -\eta_{43} & 0 \\ -\eta_{14} & 0 & -\eta_{34} & \eta_4 & -\eta_{54} \\ -\eta_{15} & -\eta_{25} & 0 & -\eta_{45} & \eta_5 \end{bmatrix} \begin{bmatrix} \omega E_1 \\ \omega E_2 \\ \omega E_3 \\ \omega E_4 \\ \omega E_5 \end{bmatrix} = \begin{bmatrix} 1 \\ 0 \\ 0 \\ 0 \\ 0 \end{bmatrix} \ . \tag{3.34}$$

The zero elements in the first left matrix representing the loss factors are the un-connected subsystems.

3.12 Calculating the Transmission Loss through duct walls

Transmission loss (TL) is the ratio of sound power incident on a partition to the transmitted sound power through the partition. TL can be influenced by the duct features (i.e. size, thickness and shape). The higher the transmission loss of the duct wall panels, lower is the sound energy passing through the duct wall. The point of interest in this study is to find the breakout sound transmission from ducts, which is the sound transmitted through the duct wall and then radiated from the exterior surface of the duct wall.

The theoretical results in ASHRAE Handbook: HVAC Applications (ASHRAE, 2011) is used to validate the results using SEA in our study. The transmission loss is evaluated as follows,

$$TL_{out} = L_{w(in)} - L_{w(out)} - 10 \log\left(\frac{S^*}{A}\right) \quad , \tag{3.35}$$

where $L_{w(in)}$ is the sound power level inside the air duct. $L_{w(out)}$ is the sound power level radiated from the outside surface of the duct walls. S^* is the effective surface area of the duct, while A is the cross sectional area of the duct. The effective surface area for the rectangular duct can be calculated by,

$$S^* = 2L^*(larger\ c/s + smaller\ c/s) \quad , \tag{3.36}$$

Where c/s is the duct cross section, L^* is the effective length of the duct which can be then calculated as,

$$L^* = \frac{\gamma_1{}^L - 1}{\ln(\gamma_1)} \quad , \tag{3.37}$$

where

$$\gamma_1 = 10^{-\frac{\alpha}{10}} \quad . \tag{3.38}$$

α is the duct attenuation rate. The duct attenuation values for the lightest gages can be extracted from the Table 48.16 of ASHRAE Handbook: HVAC Applications (ASHRAE, 2011).

3.13 Calculating the Cutoff Frequency

The cut-off frequency for the waveguide with rectangular cross section can be determined by Kinsler's (2000) formulation. It is useful in order to probe the lowest natural frequencies of the enclosed volume to validate our assumption that the fundamental resonance frequency of the plates is smaller than the lowest natural frequency of the enclosed volume. The equation for calculation of the cutoff frequencies of the duct discussed in Section 3.1 is expressed in this section.
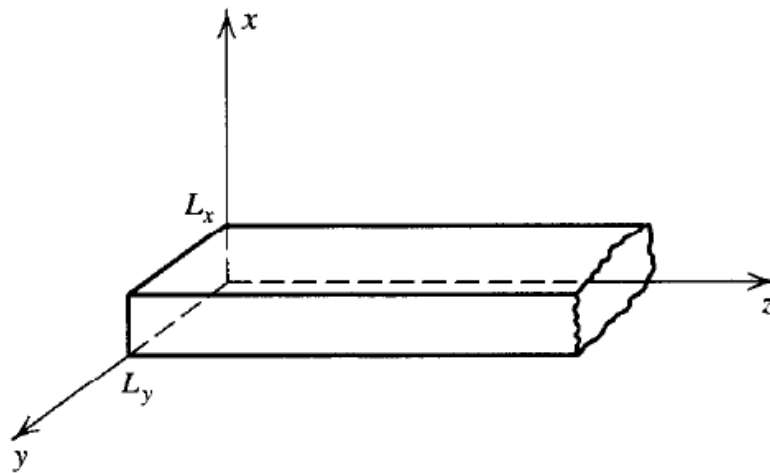
Figure 3.3 - Waveguide with dimension Lx and Ly (Kinsler, 2000).

The wavenumber for *x* and *y* axes are:

$$k_{xp} = \frac{p\pi}{L_x} \qquad p = 0,1,2,\dots \tag{3.39}$$

$$k_{yq} = \frac{q\pi}{L_y} \qquad q = 0,1,2,\dots \tag{3.40}$$

where k_{xp} and k_{yq} are the components of the wave number in x and y direction respectively. p and q are integer and the mode numbers for x and y axes, respectively. L_x and L_y represent the dimensions of the plate. The transverse component of the propagation vector for rectangular cross-section duct can be shown as follows,

$$k_{pq} = \left(k_{pq}^2 + k_{pq}^2\right)^{\frac{1}{2}}, \tag{3.41}$$

The cut-off frequency can be then found,

$$f_{pq} = \frac{ck_{pq}}{2\pi}. \tag{3.42}$$

3.14 Summary

The procedure employed by SEA to predict the transmission loss (TL) of breakout noise through air duct walls involves the evaluation of various parameters. First of all, the ductwork is divided into six subsystems: four walls (plates), one internal cavity and an external space. By making the appropriate assumptions, the loss factors are described. These involve internal loss factor for internal air volume, dissipation loss factors for the plates, coupling loss factor between the subsystems and total loss factor for each subsystem. In the process some frequencies (such as the critical frequency, the resonance frequency of the duct wall panels and the cut-off frequency of the waveguide) are also discussed to meet certain requirements and assumptions. Intrinsic parameters like radiation coefficients for coupling loss factors within duct walls and internal air volume, transmission coefficient for non-resonant coupling loss factor and modal densities to account for the remaining unknown coupling loss factors are also identified. These loss factors are then introduced in the power balance equation and the energy radiated from duct walls is

estimated. Thus, the acoustic power coming out of the ductwork is used to predict the transmission loss of breakout noise through the duct wall by employing the general formulation transmission loss (TL).

Chapter 4: Results and Analysis

4.1 Initially Predicted Results by SEA

Applying the preceding methodology discussed in Chapter 3, the sound transmission loss of the air duct for the breakout noise is predicted by statistical energy analysis (SEA) with the aid of MATLAB computer software (Appendix A). The results are then compared with the theoretical results in Chapter 48 of ASHRAE Handbook: HVAC Applications (ASHRAE, 2011) for evaluation. As stated in Section 3.1, duct of dimension 0.305 m x 0.610 m x 6.1 m is considered for the present study. The sound transmission loss (TL) based on the ASHRAE's theoretical results (ASHRAE, 2011) for the given duct size have been listed in Table 4.1 (column 2). The TL of breakout noise is stated at octave band frequencies.

The SEA method is simulated to yield the predicted transmission loss results in order to get an agreement with the theoretical results. The predicted outputs have been plotted graphically as seen in Figure 4.1. There is a good agreement of predicted values with the theoretical results at frequencies between 250 Hz and 2000 Hz. The agreement is also recorded at the lower frequencies (63 Hz and 125 Hz). However, the theoretical TL is higher than the predicted TL at frequencies above 2000 Hz. As shown in Figure 4.1, the theoretical values are significantly higher at 4000 Hz and 8000 Hz. These discrepancies at the higher frequencies defeat the purpose of the SEA as its original claim is to be accurate at higher frequencies (Heckl, 1994).
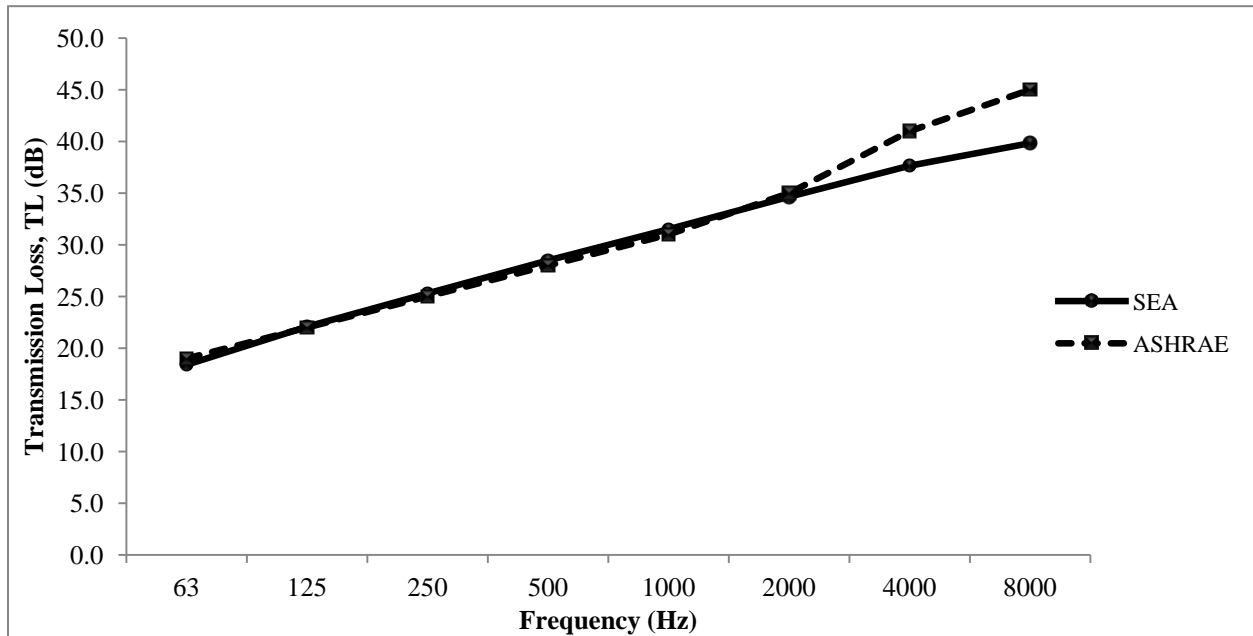
Figure 4.1 - Transmission Loss (TL) predicted by SEA and theoretical TL by ASHRAE (2011) for duct 0.305 m x 0.610 m x 6.1 m.

The numbers obtained by predicted (SEA) TL at the octave band frequencies are listed in Table 4.1. The theoretical TL values (ASHRAE, 2011) are also listed for comparison. The corresponding differences in the theoretical values and the predicted values have been shown. At frequencies 63 Hz to 2000 Hz, the deviations noticed between the predicted and theoretical are below 1 dB. The predicted results and the theoretical results at 63 to 2000 Hz follow a mass 3 dB increase in TL per doubling of frequency. The deviations of the predicted TLs are enlarged at 4 and 8 kHz, which record deviations of 3.3 dB and 5.2 dB, respectively. The theoretical TL shows a steep increase at above 4 kHz in comparison with the predicted.

Table 4.1 - Theoretical TL (ASHRAE, 2011) and the initially predicted TL using SEA for a duct 0.305 m x 0.610 m x 6.1 m.

Frequency (Hz)	ASHRAE (dB)	SEA (dB)	Deviation (dB)
63	19	18.4	0.6
125	22	22.1	-0.1
250	25	25.3	-0.3
500	28	28.5	-0.5
1000	31	31.5	-0.5
2000	35	34.6	0.4
4000	41	37.7	3.3
8000	45	39.8	5.2

4.2 Calculating the Transmission Loss using Cummings Equations (Cummings, 1985)

The phenomenon of increase in theoretical TL (ASHRAE, 2011) at higher frequencies may be explained by Cummings' theory (1985). It states that, at sufficiently high frequencies, the duct wall response to an internal plane wave is essentially given by the mass law.

The expression used to estimate the TL of a rectangular duct at lower frequencies where plane acoustic mode propagates within the duct can be stated as (Cummings, 1985),

$$TL_1 = 10\log \left[\frac{4\omega \rho_s{}^2}{\rho_0^2 c(a+b)}\right] \quad , \tag{4.1}$$

where *a* and *b* are the cross sectional dimensions of the rectangular duct. The above formulation in Equation 4.1 can be used to estimate the TL of the rectangular duct at frequencies where only plane acoustic mode propagates within the duct. Hence it poses certain limitations. It is only

valid up to $613/\sqrt{ab}$ Hz where *a* and *b* are in meters (the validity of the formulation for the current duct dimension is 1421.17 Hz). Above this frequency, more than about ten acoustic modes can propagate in the duct, which then leads to "multimodal" transmission. To overcome this, Cummings (1985) found expression for the TL using mass law (i.e. 6 dB increase every doubling for frequency) of higher order duct modes by summing the contributions from all propagating modes at any frequency. It can be stated that the statistical estimates of the internal and radiated sound power can be made by summing the contributions from all propagating modes at any frequency. The resulting TL formula was (Cummings, 1985),

$$TL_2 = 10\log \left(\frac{\rho_s^2 \omega^2}{7.5\rho_0^2 c}\right), \tag{4.2}$$

While the Equation 4.1 resulted in 3 dB/octave increase of TL for each octave band frequency, the Equation 4.2 results in 6 dB/octave increase of TL for each octave band frequency.

When the above two (i.e. Equation 4.1 and Equation 4.2) formulations were applied to our duct model as shown in Figure 4.2, the Equation 4.1 gave close predictions up to about 2 kHz. At frequencies above 2 kHz the multimodal model using Equation 4.2 with 6 dB/octave band increase of TL may show promising results and may have a better agreement with the theoretical results (ASHRAE, 2011). Figure 4.2 exhibits the behavior of plane acoustic mode propagation by applying Equation 4.1 and the higher order mode application using Equation 4.2. The magnitudes for Equation 4.1 and 4.2 have been listed for the respective octave bands in Table 4.2
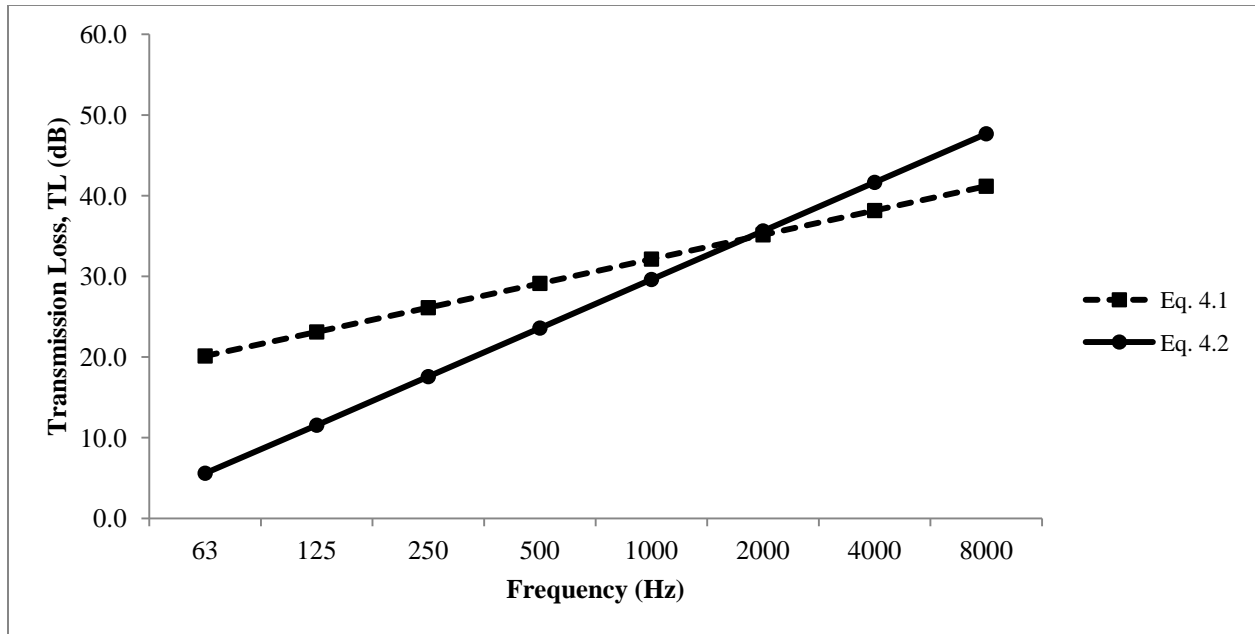
Figure 4.2 - Transmission loss with plane acoustic mode (Equation 4.1) and higher order mode (Equation 4.2) for duct 0.305 m x 0.610 m x 6.1 m.

Table 4.2 - TL for plane acoustic mode and higher order mode propagation for duct 0.305 m x 0.610 m x 6.1 m.

Frequency (Hz)	ASHRAE (dB)	Equation 4.1 TL (dB)	Equation 4.2 TL (dB)
63	19	20.1	5.6
125	22	23.1	11.5
250	25	26.1	17.6
500	28	29.1	23.6
1000	31	32.1	29.6
2000	35	35.1	35.6
4000	41	38.2	41.6
8000	45	41.2	47.7

Table 4.2 compares the values of the theoretical TL (ASHRAE, 2011) with the predicted TL obtained by Equations 4.1 and 4.2 respectively. It can be clearly seen that the results based on the plane wave mode model using Equation 4.1 which show an increase in 3 dB/octave. The higher order modes model using Equation 4.2 follow the mass law showing an increase of 6 dB/octave. The theoretical data (ASHRAE, 2011) is in close agreement with plane acoustic mode propagation (Equation 4.1) from frequencies 63 Hz to 2000 Hz, while the higher order mode propagation (Equation 4.2) comes in close agreement at frequencies 4000 Hz and 8000 Hz with the theoretical results.

4.3 Evaluating the Correction Factor

As shown in Figure 4.2, the predicted TL using the plane acoustic mode model intersect with that using the higher order mode model at a particular frequency, which we term as a "transition frequency" in the present study. Above this frequency, the transmission loss in the duct would be dominated by the higher order mode. We find this transition frequency by equating Equations 4.1 and 4.2

$$\left[\frac{4\omega\rho_s{}^2}{\rho_0^2 c(a+b)}\right] = \left(\frac{\rho_s{}^2\omega^2}{7.5\rho_0^2 c}\right) . \tag{4.3}$$

The formulation for the transition frequency is shown below in Equation 4.4,

$$f_t = \frac{30c}{2\pi(a+b)} , \tag{4.4}$$

where f_t is the transition frequency.

The purpose of calculating the transition frequency is to be able to apply a correction factor from a point where higher order modes propagation is dominated. Hence, we propose to apply a correction factor above the transition frequency to account for the higher order mode propagation. The correction factor is based on the difference between Cummings' TL equations for higher order modes (Equation 4.2) and for plane acoustic wave mode (Equation 4.1) as,

$$TL_2 - TL_1 = 10\log\left(\frac{2\pi f(a+b)}{30c}\right) \quad . \tag{4.5}$$

Therefore, for $f > f_t$, the transmission loss will be,

$$TL_{f_t} = TL + 10\log\left(\frac{2\pi f(a+b)}{30c}\right), \tag{4.6}$$

where TL_{f_t} is the transmission loss above the transition frequency and TL can be found by Equation 3.35. The transition frequency f_t for our duct dimension is 1.78 kHz. The revised formulation of TL in Equation 4.6 has a good agreement at the higher order mode propagation as shown in the following section.

4.4 Improvement in Prediction of Transmission Loss (TL) using Equation 4.6.
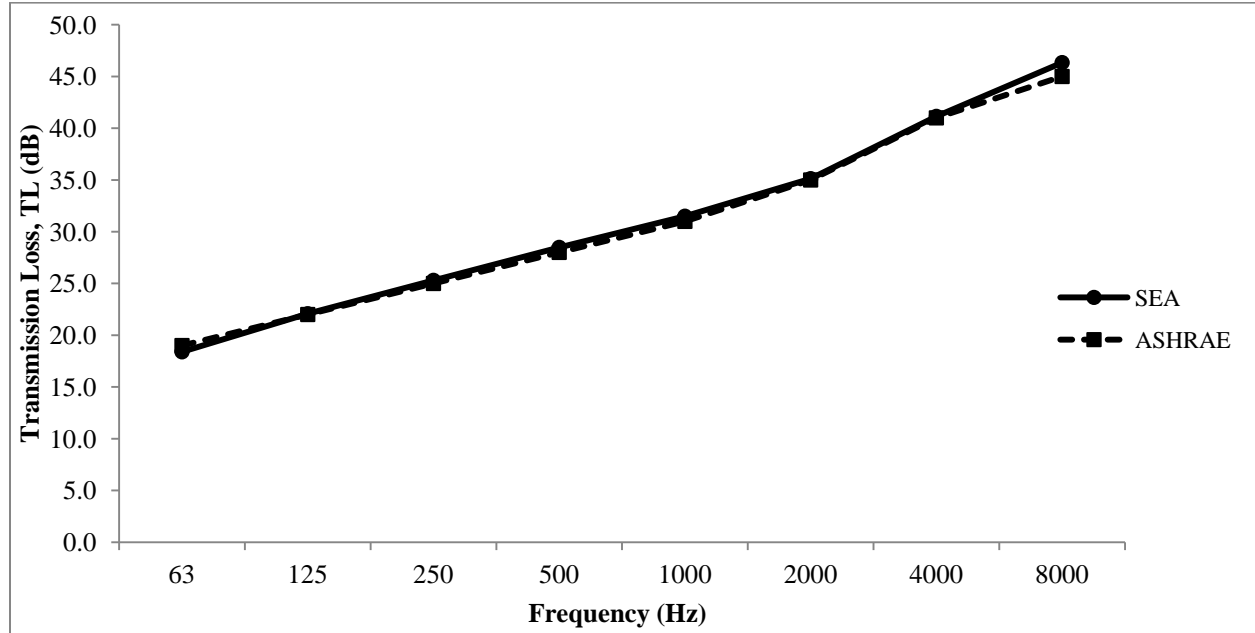
Figure 4.3 - Predicted TL with correction factor from Equation 4.5 above the transition frequency and the theoretical TL for duct 0.305 m x 0.610 m x 6.1 m.

Figure 4.3 shows the breakout TL for our duct after applying the correction factor above the transition frequency. As seen, there is a close agreement after accounting for the higher order modes at the frequencies above transition frequency, specifically at frequencies 2000 Hz, 4000 Hz and 8000 Hz. As the higher order modes propagate, the predicted TL follows the same nature of the theoretical TL (ASHRAE, 2011) and is within 2 dB of deviation.

Table 4.3 shows the magnitude of the breakout TL obtained after applying the correction factor at frequencies above the transition frequency. By comparing it with earlier results listed in Table 4.2, the deviations at the high frequencies 2000 Hz, 4000 Hz and 8000 Hz are reduced significantly. The deviations from the improved predicted results are 0.1, 0.1 and 1.3 dB for frequencies 2000, 4000 and 8000 Hz respectively, as compared with 0.4, 3.3 and 5.2 dB in Table

4.2 using the original equation. The newly predicted results are well within 2 dB of agreement with the theoretical results.

Table 4.3 - Predicted TL values (with revised formulation) and theoretical TL values for duct 0.305 m x 0.610 m x 6.1 m.

Frequency (Hz)	ASHRAE (dB)	SEA (dB)	Deviation
63	19	18.4	0.6
125	22	22.1	-0.1
250	25	25.3	-0.3
500	28	28.5	-0.5
1000	31	31.5	-0.5
2000	35	35.1	-0.1
4000	41	41.1	-0.1
8000	45	46.3	-1.3

4.5 Contributions of Resonant and Non-Resonant Responses to the TL of the Duct Walls

The spectrum of analysis is further stretched to study the TL contributed by the resonant and non–resonant responses. The excitation caused by the acoustic waves and the total vibration energy can be divided into two parts. The first is the forced response, also called the non-resonant response, which adds to the non-resonant sound transmission. The second part is generated from the free response acting in the form of resonant modes and inducing resonant sound transmission (Lei et al, 2011). The resonant response is by the structural modes caused by the interaction of the free bending waves with the boundaries of the structure while the non-

resonant response is due to the trace wave (moving along the surface of the duct walls) generated in the panel by the incident acoustic excitation field.
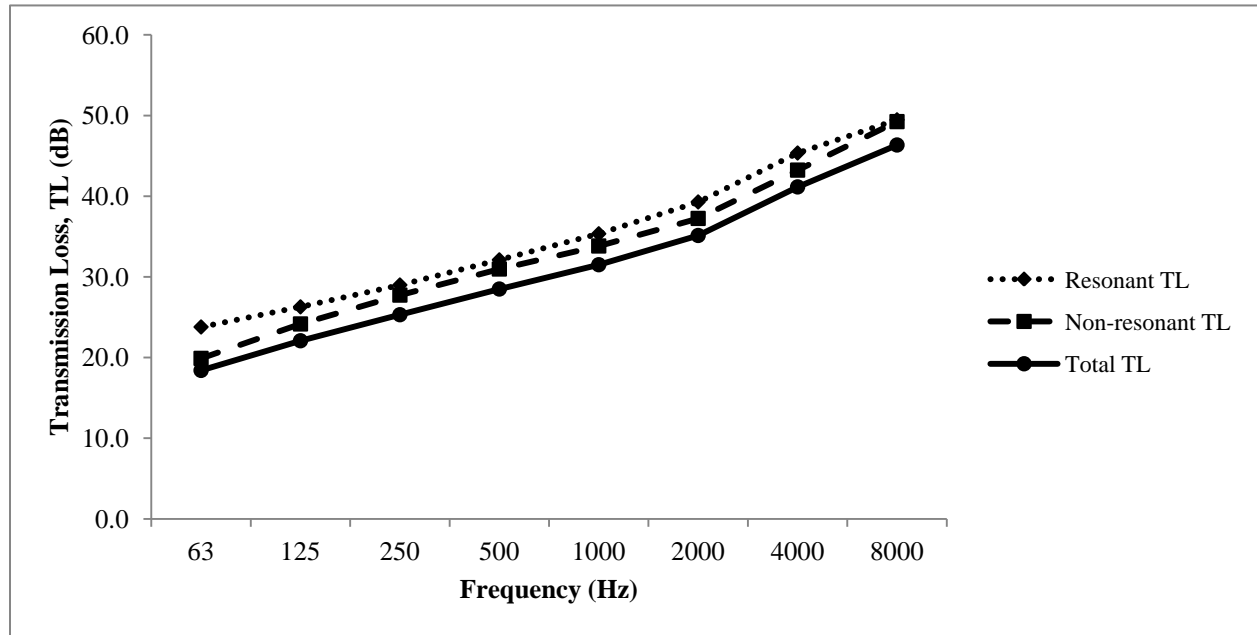
Figure 4.4 - Predicted resonant TL and non-resonant TL for duct 0.305 m x 0.610 m x 6.1 m.

Figure 4.4 shows the transmission losses by the resonant response and the non-resonant response along with the total transmission loss that is the sum of the transmission losses contributed from the resonant and non-resonant parts. As shown in Figure 4.4, the transmission loss contributed by the resonant response is higher than the non-resonant response throughout the octave bands. Hence, it can be commented that the power transmitted by the resonant response is less than that of the non-resonant response at the above given frequency range, which will be shown in the preceding section (Section 4.5). The values of the predicted resonant TL and non-resonant TL have been listed in Table 4.4. The difference of TL contribution from the resonant over the non-resonant is around 2 to 4 dB over the octave band center frequencies.

Table 4.4 - Predicted Resonant and Non-Resonant response values duct 0.305 m x 0.610 m x 6.1 m.

Frequency (Hz)	Resonant TL (dB)	Non-Resonant TL (dB)	Total TL (dB)
63	23.8	19.9	18.4
125	26.3	24.2	22.1
250	29.0	27.7	25.3
500	32.1	31.0	28.5
1000	35.3	33.8	31.5
2000	39.3	37.2	35.1
4000	45.3	43.2	41.1
8000	49.5	49.2	46.3

4.6 Sound Power Level Transmitted Out of the Air Duct by Resonant and Non-Resonant Responses.

The predicted sound power level coming out of the air duct will be the contibutions by the resonant sound power level and the non-resonant sound power level.

$$Total\ Sound\ PowerLevel_{out} = Reso.Sound\ Power\ Level + NonReso\ Sound\ Power\ Level$$

(4.7)
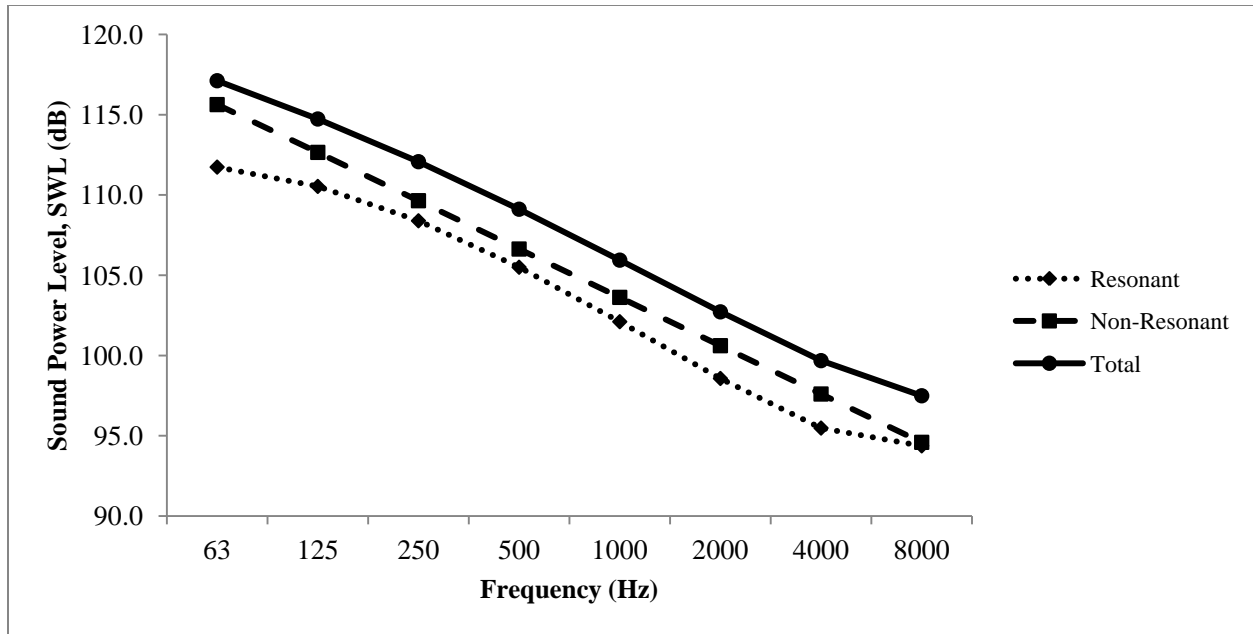
Figure 4.5 - Predicted resonant and non-resonant transmitted Sound Power Level (SWL) for duct 0.305 m x 0.610 m x 6.1m.

As shown in Figure 4.5, the non-resonant response dominates the acoustic energy transmitted through panels in our case, which results in the Sound Power Level (SWL) out due to the non-resonant response to be more dominant than the resonant response. Thus, the non-resonant response is responsible for major SWL transmission from the duct panels as compared to the resonant response.

Table 4.5 shows the magnitudes of SWL transmitted through the air duct walls by the resonant and non-resonant responses. The non-resonant mechanism dominates SWL transmission over the octave band frequency under study. The dominating difference varies from as low as 0.2 dB to as high as 3.9 dB at different center frequencies of the octave bands.

Table 4.5 - Predicted values for resonant and non-resonant transmitted SWL for duct 0.305 m x 0.610 m x 6.1 m.

Frequency (Hz)	Resonant SWL (dB)	Non-Resonant SWL (dB)	Total SWL (dB)
63	111.7	115.6	117.1
125	110.5	112.7	114.7
250	108.4	109.6	112.1
500	105.5	106.6	109.1
1000	102.1	103.6	105.9
2000	98.6	100.6	102.7
4000	95.5	97.6	99.7
8000	94.4	94.6	97.5

4.7 Resonant and Non-Resonant Responses Near to and Above Critical Frequency

In general, the transmitted sound power level by resonant response is very low at frequencies below the critical frequency of the duct panel and is high at the frequencies near and above the critical frequency. This is because the radiation efficiency linked to resonant response is small below the critical frequency (Renji and Nair, 2001). This results from the wavelength of resonant response being shorter than that of sound in air; hence the resonance response is an inefficient radiator (Lei et al, 2011). However, the sound radiation from resonant response gets dominant at frequencies near and above critical frequency.

For the chosen duct dimension, this theory can be verified by evaluating the resonant and non-resonant TL near and above the critical frequency. The critical frequency of the duct panels is 16.9 kHz.
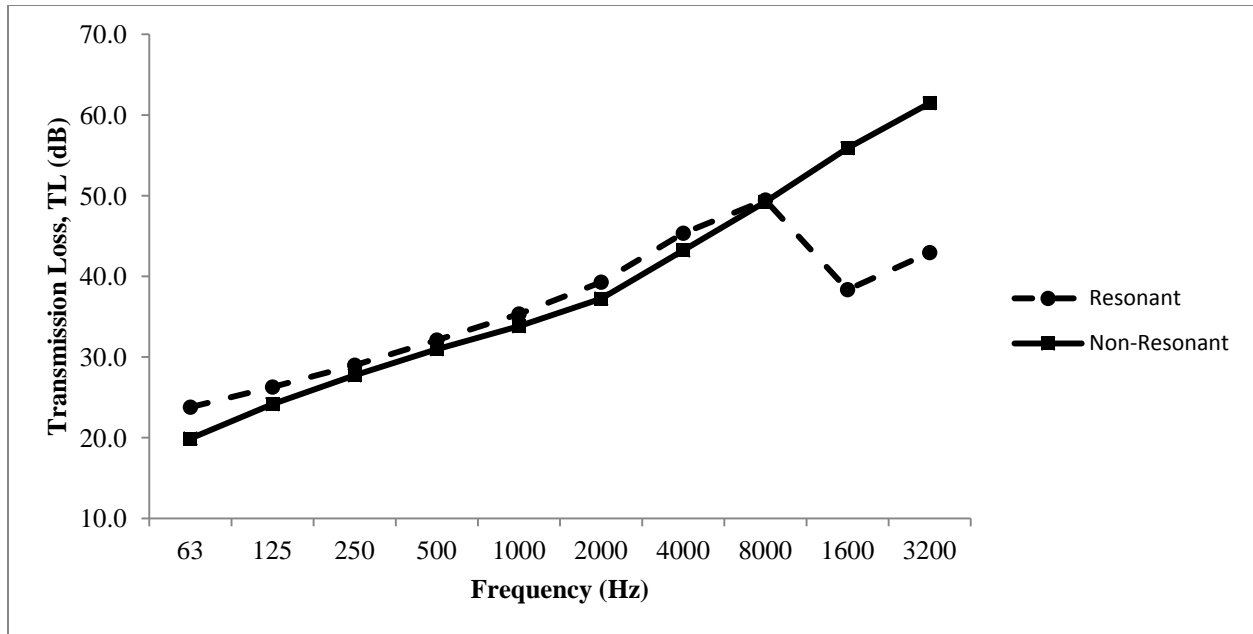
Figure 4.6 - Predicted resonant and non-resonant TL extended to the frequencies above the critical frequency for duct 0.305 m x 0.610 m x 6.1 m.

In Figure 4.6, high TL of the breakout noise due to the resonant response can be observed up to a certain frequency, after which it shows a decline and falls significantly below that of the non-resonant response. On the other hand, the TL due to the non-resonant response at the frequencies below the critical frequencies is lower than that due to resonant response. High TL due to non-resonant response can be observed near and above the critical frequency.

The same concept in terms of sound power level transmitted out above the critical frequency can be explained by the dominance of non-resonant response below the critical frequency and then being dominated by the resonant response at higher frequencies as shown in Figure 4.7. Hence it can be said that generally, the sound power level transmission is dominated by the non-resonant response below the critical frequency. As frequency approaches the critical frequency, there is an increase in radiation from the resonant response thereby dominating the acoustic power transmission.
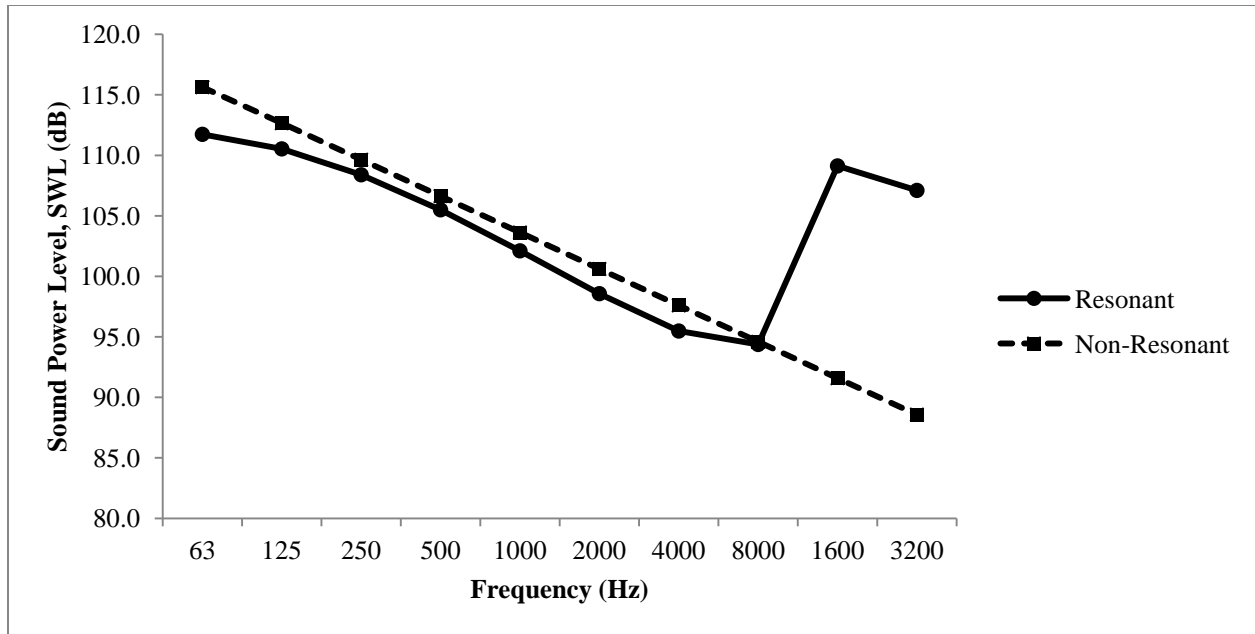
Figure 4.7 - Predicted SWL for resonant and non-resonant responses extended to the frequencies above the critical frequency for duct 0.305 m x 0.610 m x 6.1 m.

To further evaluate our SEA method, we randomly select three more dimensions with different each with different gages and covering the maximum and minimum (0.305 m and 2.44 m respectively) cross sectional dimension stated in the ASHRAE Handbook: HVAC Applications (ASHRAE, 2011) and check the agreement between the predicted results and the theoretical results. The transmission loss of the breakout noise for all the three duct dimensions each with different gages are predicted and are shown in Figures 4.8, 4.9 and 4.10 The magnitude of the transmission losses are listed in Tables 4.6, 4.7 and 4.8.

4.8 Predicted TL values for duct 0.610m x 0.610m x 6.1m

Figure 4.8 - Predicted and theoretical TL for duct 0.610 m x 0.610 m x 6.1m.

Figure 4.8 shows the graphical representation of the predicted TL in comparison with theoretical TL for duct dimension 0.610 m x 0.610 m x 6.1 m with 22-gage (0.853 mm) duct walls. As seen, the predicted TL follows close to the theoretical TL over the given frequency range. The numeric values have been listed in Table 4.6. The deviations are large at the lower frequencies (63 Hz and 125 Hz). However, from the intermediate to high frequencies (250 Hz to 8000 Hz), the deviations are within 2 dB. The large deviation at the lower frequency are expected as SEA has limitations at the lower frequencies and is predominantly meant to generate stable results at the higher frequencies (Sarradj, 2004).

Table 4.6 - Predicted and theoretical TL values and corresponding differences for duct 0.610 m x 0.610 m x 6.1 m.

Frequency (Hz)	ASHRAE (dB)	SEA (dB)	Deviation (dB)
63	20	17.3	2.7
125	23	21.0	2.0
250	26	24.4	1.6
500	29	27.8	1.2
1000	32	30.9	1.1
2000	37	35.8	1.2
4000	43	41.7	1.3
8000	45	46.3	-1.3

4.9 Predicted TL values for duct 0.610m x 1.22m x 6.1m

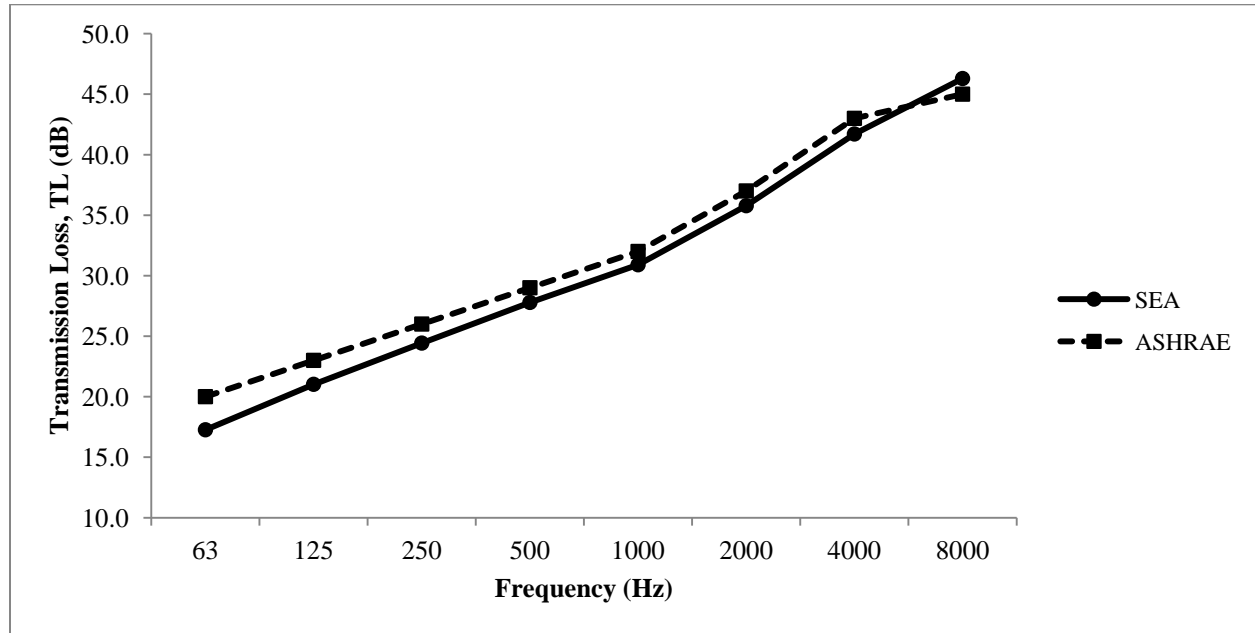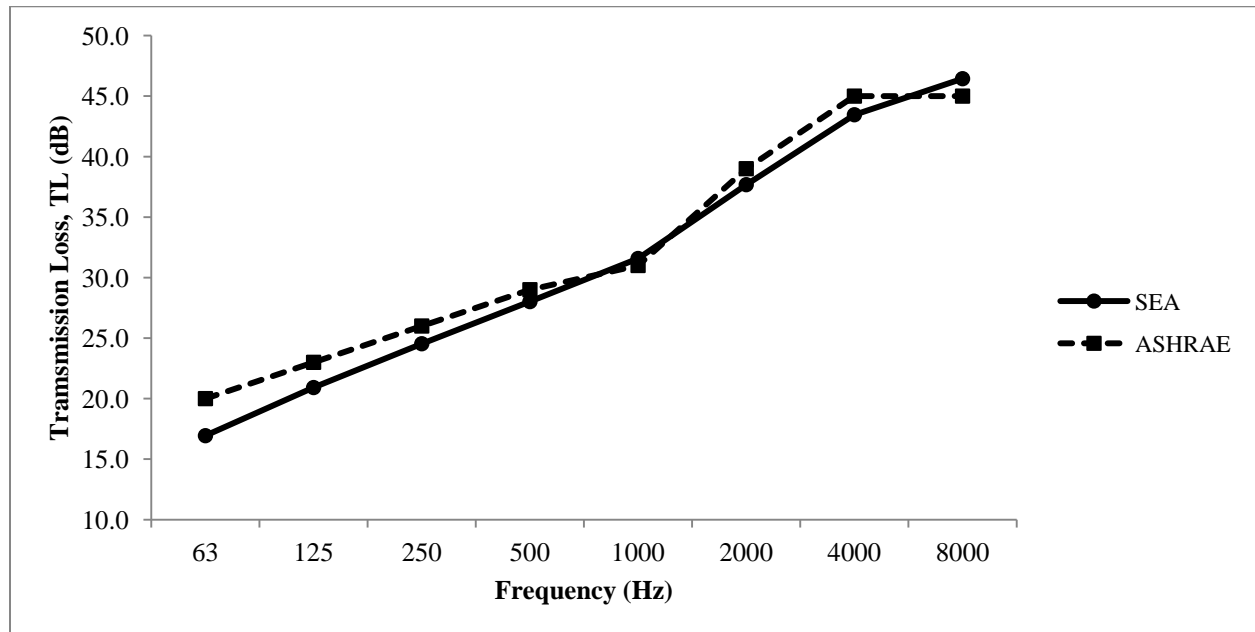Figure 4.9 - Predicted and theoretical TL for duct size 0.610 m x 1.22 m x 6.1 m.

Figure 4.9 shows the graphical representation of the predicted TL in comparison with theoretical TL for duct dimension 0.610m x 1.22m x 6.1m for 20-gage (1.066 mm) duct walls. The predicted TLs follow closely to the theoretical TL over the frequency range in the present study. The numeric values have been listed in Table 4.7. The predicted values are seen to be in agreement from intermediate to the high frequencies (250 Hz to 8000 Hz) within 2 dB deviations.

Table 4.7 - Predicted and theoretical TL values and corresponding differences for duct 0.610 m x 1.22 m x 6.1 m.

Frequency (Hz)	ASHRAE (dB)	SEA (dB)	Deviation (dB)
63	20	16.9	3.1
125	23	20.9	2.1
250	26	24.5	1.5
500	29	28.0	1.0
1000	31	31.6	-0.6
2000	39	37.7	1.3
4000	45	43.5	1.5
8000	45	46.4	-1.4

4.10 Predicted TL values for duct 1.22m x 2.44 m x 6.1m
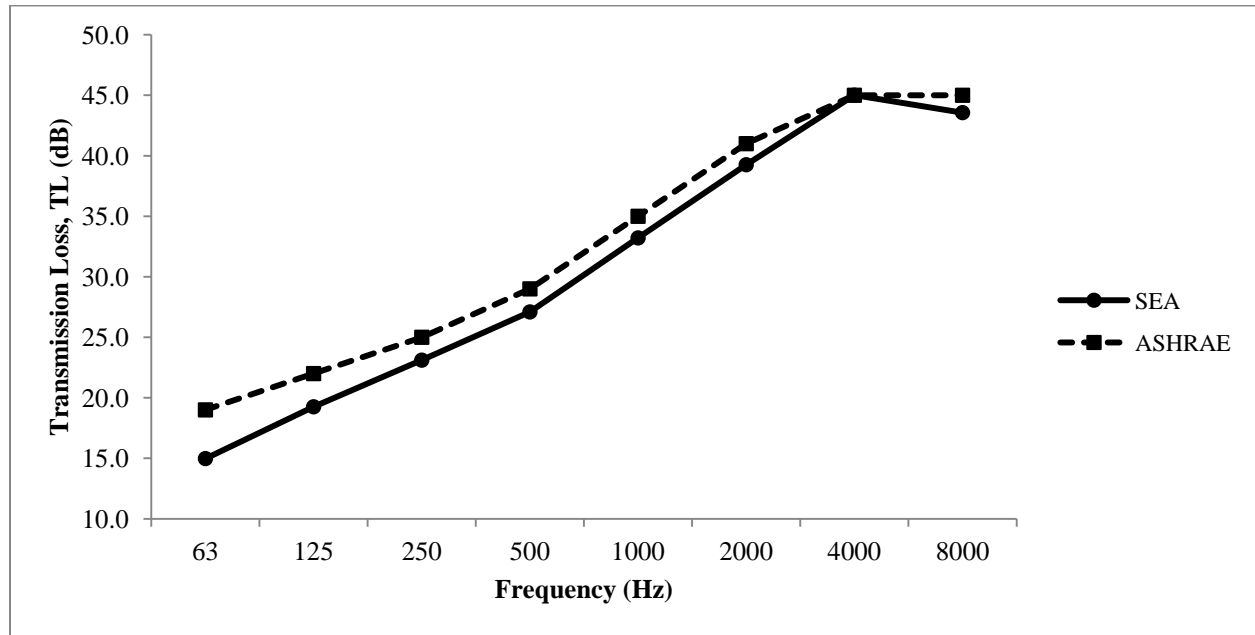
Figure 4.10 - Predicted and theoretical TL for duct 1.22 m x 2.44 m x 6.1 m.

Figure 4.10 displays the predicted and theoretical TL for cross-sectional duct dimension 1.22m x 2.44m x 6.1m with 18-gage (1.311 mm) duct walls. Observed again is a close proximity of the predicted results with the theoretical results. Table 4.8 lists the values obtained for the predicted TLs to compare it with the theoretical TLs. The highest deviation at mid to high frequencies are 1.9 dB at 250 and 500 Hz, which also fall below 2 dB. It can be concluded that predictions using SEA are close to the theoretical values.

Table 4.8 - Predicted and theoretical TL values and corresponding differences for duct 1.22 m x 2.44 m x 6.1 m.

Frequency (Hz)	ASHRAE (dB)	SEA (dB)	Deviation (dB)
63	19	15.0	4.0
125	22	19.3	2.7
250	25	23.1	1.9
500	29	27.1	1.9
1000	35	33.2	1.8
2000	41	39.3	1.7
4000	45	45.0	0.0
8000	45	43.6	1.4

4.11 Predicted TL values for all other standard dimensions as listed in ASHRAE

Table 4.9 – Results for duct 0.305 m x 0.305 m x 6.1 m

Frequency (Hz)	ASHRAE (dB)	SEA (dB)	Deviation (dB)
63	21	19.5	1.5
125	24	22.9	1.1
250	27	25.7	1.3
500	30	28.6	1.4
1000	33	31.4	1.6
2000	36	34.5	1.5
4000	41	39.2	1.8
8000	45	44.2	0.8

Table 4.10 - Results for duct 0.305 m x 1.22 m x 6.1 m

Frequency (Hz)	ASHRAE (dB)	SEA (dB)	Deviation (dB)
63	19	18.0	1.0
125	22	22.0	0.0
250	25	25.6	-0.6
500	28	29.0	-1.0
1000	31	32.0	-1.0
2000	37	37.8	-0.8
4000	43	43.8	-0.8
8000	45	47.8	-2.8

Table 4.11 - Results for duct 0.305 m x 1.22 m x 6.1 m

Frequency (Hz)	ASHRAE (dB)	SEA (dB)	Deviation (dB)
63	21	19.8	1.2
125	24	22.3	1.7
250	27	25.2	1.8
500	30	28.3	1.7
1000	35	33.1	1.9
2000	41	39.1	1.9
4000	45	44.7	0.3
8000	45	42.1	2.9

As seen in Tables 4.9, 4.10 and 4.11, the predicted results follow close to the theoretical values from the mid to high frequency (250 Hz to 8000 Hz). The observed agreement is within 3 dB.

4.12 Predicted TL Values Compared with the Experimental Data from Cummings (1983a)
report

The predicted values are compared with the experimental TL data for a simple rectangular cross-

sectional duct dimensions from Cummings' Report (Cummings, 1983a).
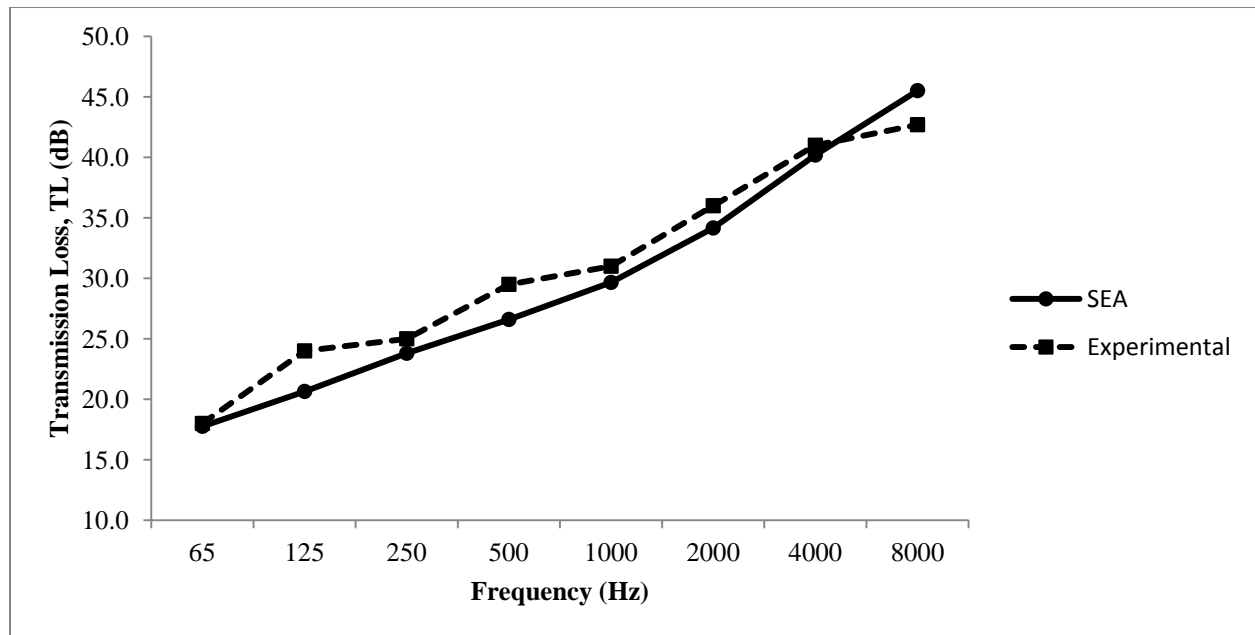
Figure 4.11 - Predicted and experimental TL for duct 0.762 m x 0.356 m x 4.57 m

Seen in Figure 4.11, the predicted TL appear to be in close agreement of the experimental data

for a simple rectangular duct dimension of 0.762 m x 0.356 m x 4.57 m for 24-gage. The

recorded deviations from the mid to the high frequency are within 3 dB of agreement as seen in

Table 4.12.

Table 4.12 - Predicted and experimental TL values and corresponding differences for duct 0.762 m x 0.356 m x 4.57 m

Frequency (Hz)	Experimental (dB)	SEA (dB)	Deviation (dB)
65	18	17.8	0.2
125	24	20.6	3.4
250	25	23.8	1.2
500	29.5	26.6	2.9
1000	31	29.7	1.3
2000	36	34.2	1.8
4000	41	40.2	0.8
8000	42.7	45.5	-2.8

Validating SEA for another duct with dimension 0.229 m x 0.152 m x 4.57 m.
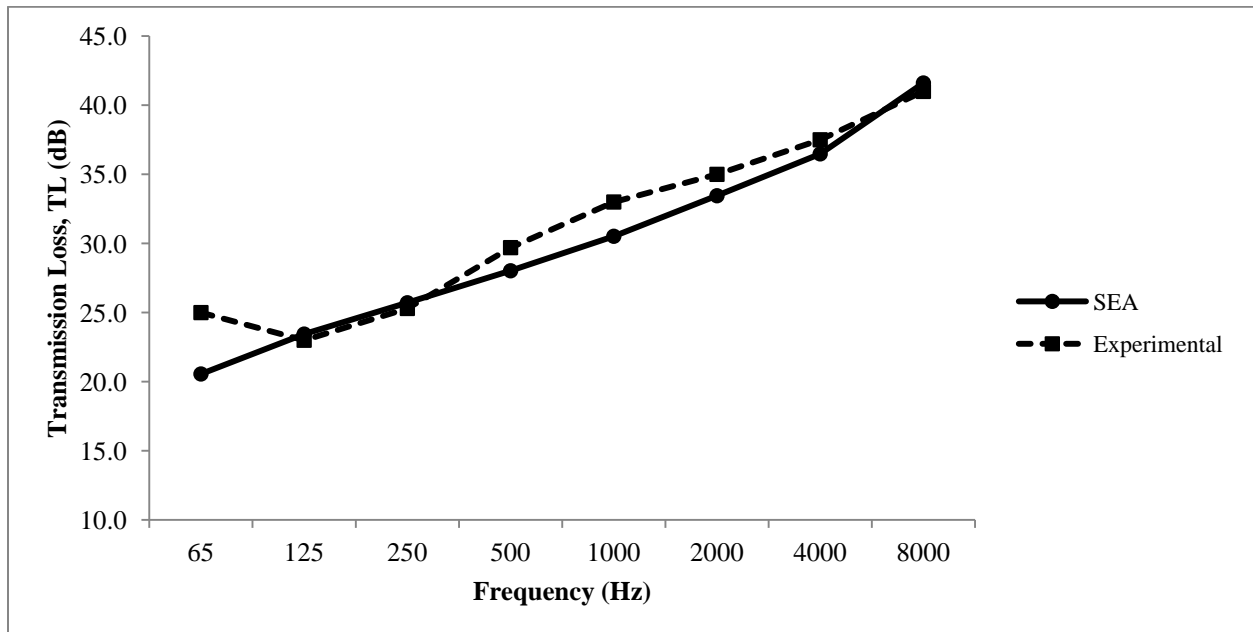
Figure 4.12 - Predicted and experimental TL for duct 0.229 m x 0.152 m x 4.57 m

Figure 4.12 compares the predicted TL results with the experimental data for the stated duct

dimension. The predicted results are again seen in close agreement with experimental data from

mid to high frequency. The results are tabulated in Table 4.13 along with their corresponding

differences.

Table 4.13- Predicted and experimental TL values and corresponding differences for duct 0.229 m x 0.152 m x 4.57 m

Frequency (Hz)	Experimental (dB)	SEA (dB)	Deviation (dB)
65	25	20.6	4.4
125	23	23.4	-0.4
250	25.3	25.7	-0.4
500	29.7	28.0	1.7
1000	33	30.5	2.5
2000	35	33.5	1.5
4000	37.5	36.5	1.0
8000	41	41.6	-0.6

As shown in the Table 4.13, the predicted TL values for duct 0.229 m x 0.152 m x 4.57 m are

within 3 dB of agreement with the experimental data.

The SEA validation is stretched to compare the experimental data for two more different cross

sectional dimensions which meet the criteria of a simple rectangular air duct geometry from

Cummings Report (Cummings, 1983a). Table 4.14 and 4.15 list the predicted TL with the

corresponding deviation from the experimental data for the given dimensions. The deviations

observed in Table 4.14 are within 3 dB of agreement. The deviations recorded for duct 0.762 m x

0.762 m x 4.57 m in Table 4.15 are mostly within 3 dB, with an exception at 1000 Hz which

records 3.4 dB.

Table 4.14 - Results for duct 0.457 m x 0.229 m x 4.57 m

Frequency (Hz)	Experimental (dB)	SEA (dB)	Deviation (dB)
65	21.9	21.0	0.9
125	23.5	22.9	0.6
250	26.6	25.4	1.2
500	29.4	27.9	1.5
1000	32.3	30.9	1.4
2000	35.4	34.0	1.4
4000	37.5	39.2	-1.7
8000	41.5	44.2	-2.7

Table 4.15 - Results for duct 0.762 m x 0.762 m x 4.57 m

Frequency (Hz)	Experimental (dB)	SEA (dB)	Deviation (dB)
65	16.9	15.6	1.3
125	22.2	18.4	3.8
250	24.5	21.7	2.8
500	28.9	25.5	3.4
1000	28.9	28.3	0.6
2000	31.5	34.1	-2.6
4000	41	40.2	0.8
8000	42.2	45.0	-2.8

4.13 Summary

The methodology discussed in Chapter 3 is applied to predict the breakout sound transmission loss for chosen duct configurations from ASHRAE Handbook: HVAC Applications (ASHRAE, 2011). The predicted results based on the methodology are then compared with the theoretical results (ASHRAE, 2011) for verification at octave band frequencies. Initially it is observed that there is close agreement of the predicted and theoretical TL results at mid frequencies only. At the higher frequencies, there are however discrepancies and the deviation from the predicted and theoretical are significant. To fix this issue, we look into Cummings earlier work on predicting the breakout sound transmission loss of air ducts (Cummings, 1985). The idea of plane propagating mode and higher order mode theory is applied to the existing methodology for development of correction factors. The newly predicted results with the proposed formulation then come in close agreement with the theoretical results i.e. with 3 dB of tolerance. To validate the SEA approach, we compare the predicted results with the experimental data borrowed from Cummings' report (Cummings, 1983a). The predicted TL results are then compared with their corresponding experimental results. The SEA predicted results are observed to be consistently in close agreement with the experimental results from the mid to the high frequency range.

Chapter 5: Conclusions

5.1 SEA's Applicability

Statistical Energy Analysis (SEA) was evaluated to predict the Sound Transmission Loss (Breakout noise) through an air duct of assorted dimensions which were taken from ASHRAE Handbook: HVAC Applications (2011). Initially, the reference held for comparing the predicted sound transmission loss was the theoretical data from ASHRAE Handbook: HVAC Application (2011) at octave band frequencies.

When SEA was applied to predict the sound transmission loss (breakout noise) for a given duct dimension, the predicted results were in close agreement with the theoretical data published in ASHRAE (2011). The deviations between the prediction by SEA and the theoretical sound transmission losses are less than 3 dB with the proposed formulation. A correction factor is proposed to improve the prediction at higher frequencies due to the higher order modes sound transmission. The predicted transmission loss follows the theoretical transmission loss closely from mid-frequency to higher frequencies (250 Hz to 8000 Hz) with the proposed SEA formulation. The application of SEA is further extended to compare the predicted results with the experimental data from Cummings' report (Cummings, 1983a). The agreement between the predicted and the experimental data was mostly observed to be within 3 dB.

SEA proved to be effective for prediction of sound transmission loss at all given dimensions and maintained a close agreement with the theoretical and experimental sound transmission loss results published earlier. SEA affirms its idea of being reasonably accurate for mid to higher frequency (250 Hz to 8 kHz) wave propagation. It can be concluded that SEA is expeditiously capable of predicting the values for sound transmission loss of any given air duct.

Though the discrepancies in the predicted results from mid to high frequency range were mostly within 3 dB, such discrepancies could be attributed to the boundary condition of the SEA model which may vary with the real model or with the measurement points which may not be stochastically selected for the real model.

5.2 Advantages of using Statistical Energy Analysis (SEA)

In ASHRAE Handbook: HVAC Applications (ASHRAE, 2011), the Transmission Loss calculated for the breakout noise was restricted to certain dimensions. SEA is potentially capable of predicting the TL for any given dimensions of the duct and gage (thickness) of the duct walls, which overcome the limitation of this theoretical data provided by ASHRAE with limited number of configurations. Besides the advantages of variations of duct dimensions and thickness, SEA is also receptive to change in duct materials. In addition, SEA also extends its capability for predicting results at much higher frequencies which is computationally difficult by other numerical methods, for instance, finite element methods (Delaere et al.,1999).

5.3 Limitations of Statistical Energy Analysis (SEA)

The main limitation of SEA is that it is still not accurate to predict the sound transmission loss at very low frequencies. It was observed that there were significant discrepancies at the frequencies below 250 Hz. SEA also failed to predict modes or mode shapes. It was unable to predict the excitation at specific frequencies either. Moreover, the modeling approach was also incompatible to FEM/BEM methods

5.4 Future Research

At higher frequencies for some models, the deviations of the predicted sound transmission losses from the theoretical results were observed to be noticeable. One of the possible reasons would be the non-diffuse field inside the air cavity of the duct. If the non-diffuse field can be considered along waveguide, the deviations may be improved.

The waveguide was considered as an enclosed volume of air for which the formulation of modal density for an enclosed cavity was employed in this approach. If a more compatible modal density equation for the waveguide can be formulated, there may be chances of reducing the deviations in the predicted results from the theoretical results.

The discrepancies of the predicted results often get enlarged at the lower frequencies where FEM/BEM methods prove effective. If prediction at these frequencies can be improved, SEA can serve as a useful tool over the entire frequency range.

To further stretch its application, SEA can be tried on round ducts, which would require a finer discretization of the duct model because of its curved geometry resulting in an increased number of subsystems and making the problem more complex.

5.5 Summary

SEA proved to be successful in predicting the sound transmission loss for the breakout noise through the rectangular ducts. The predicted (SEA) results were in close agreement with the theoretical (ASHRAE, 2011) results and experimental data (Cummings, 1983a) mostly within 3 dB of deviation from the mid to high frequency range (250 Hz to 8 kHz). At the lower frequencies (63 Hz and 125 Hz), though, the discrepancies were significant for some models,

SEA still served as a useful tool for high frequency prediction as it originally claimed. There is still wide scope to improve the predicted results especially at lower frequencies. The SEA predicting technique can also be proposed to study complex geometries of ducts like flat oval duct or circular duct where discretization could pose a great challenge.

References

ASHRAE (2011). Noise and Vibration Control (Chapter 48). *ASHRAE Handbook: Heating, Ventilation and Air Conditioning Applications*.

ASHRAE (2012). Duct Construction (Chapter 19). *ASHRAE Handbook: HVAC Systems and Equipment.*

Belyaev, A. (1993). High frequency vibration of extended complex structures. *Probabilistic Engineering Mechanics.* 8, 15-24.

Beranek, L. and Ver, I. (1992). Noise and vibration control engineering. Principles and application. *New York: J. Wiley and Sons.*

Bies, D. (1980). In situ determination of loss and coupling loss factors by the power injection method. *Journal of Sound and Vibration.* 70 (2), 187-204.

Burkett, C. (2007). Freightliner Uses Statistical Energy Analysis to Create the Quietest Truck Cab. Product Validation/Engineering Analysis, *Freightliner LLC, Portland, Oregon.*

Burrough C., Fisher R. and Kern F. (1997). An introduction to statistical energy analysis. *Journal of the Acoustical Society of America.* 101(4), 1779-1789.

Craik, R. (1996). Sound transmission through buildings using Statistical Energy Analysis. *Gower Publishing Limited, Hampshire, England.*

Cummings, A. (1975a). Sound transmission in a folded angular duct. *Journal of Sound and Vibration.* 41 (3), 375-379.

Cummings, A. (1975b). Sound transmission in 180° duct bends of rectangular section. *Journal of Sound and Vibration.* 41, 321-334.

Cummings, A. (1978). Sound generation and transmission flow ducts with axial temperature gradients. *Journal of Sound and Vibration*. 57 (2), 261-279.

Cummings, A. (1979). The attenuation of lined plenum chambers in ducts, measurement and comparison with theory. *Journal of Sound and Vibration*. 63 (1), 19-32.

Cummings, A. (1980). Low frequency acoustic radiation from duct walls. *Journal of Sound and Vibration*. 71 (2), 201-226.

Cummings, A. (1981). Design charts for low frequency acoustic transmission through the walls of rectangular ducts. *Journal of Sound and Vibration*. 78 (2), 269-289.

Cummings, A. (1982). A comparison of measured and computed sound pressure levels in a non-uniform acoustically lined duct. *Journal of Sound and Vibration*. 85 (3), 407-414.

Cummings, A. (1983a). Acoustic noise transmission through the walls of air –conditioning ducts. Final Report. *Department of Mechanical and Aerospace Engineering, University of Missouri, Rolla.*

Cummings, A. (1983b). Approximate asymptotic solutions for acoustic transmission through the walls of rectangular duct. *Journal of Sound and Vibration*. 90 (2), 211-227.

Cummings, A. (1983c). Higher order mode acoustic transmission through the walls of rectangular ducts. *Journal of Sound and Vibration*. 90 (2), 193-209.

Cummings, A. (1985). Acoustic noise transmission through duct walls. *ASHRAE transactions*. 48-61.

Cummings, A. (2001). Sound transmission through duct walls. *Journal of Sound and Vibration*. 239 (4), 731-765.

Delaere, K., Iadevavia, M., Heylen, W., Paul, S., Hameyer, K. and Belmans, R. (1999). Statistical energy analysis of acoustic noise and vibration of electric motors: transmission from air gap field to motor frame. *Conference record of the IEEE*. 3, 1897-1902.

Eichler, E. (1965). Thermal circuit approach to vibrations in coupled systems amd noise reduction of a rectangular box. *Journal of the Acoustical Society of America*. 37 (6), 995-1007.

Fahy, F. (1994). Statistical energy analysis: a critical overview. *Phil. Trans. R. Soc. Lond. A*. 346, 431-447.

Fahy, S. (2004). A note on the subdivision of a volume of air in a vehicle enclosure into sea subsystems. *Journal of Sound and Vibration*. 271 (2004), 1170-1174.

Guasch, O and Cortes, L. (2009). Graph theory applied to noise and vibration control in statistical energy analysis models. *Journal of the Acoustical Society of America*. 125(6), 3657-3672.

Guthrie, A. (1979). Low frequency acoustic transmission through the duct walls of various types of ducts. *Polytechnic of the South Bank M.Sc. Dissertation*.

Hambric, S. (2000). Structural Acoustics Literature. *ASME IMECE*.

Heckl, M. and M. Lewit. (1994). Statistical energy analysis as a tool for quantifying sound and vibration transmission paths. *Phil. Trans. R. Soc. Lond. A*. 346, 449-464.

Kinsler, L. (2000). Fundamentals of Acoustics. Fourth edition. *Libaray of Congress Cataloging-in-publication Data*.

Kuttruff, H. (1979). Room Acoustics. 2nd ed. *Applied Science Publishers, London*.

Langley, R. (1990). Elastic wave transmission through plate/beam junctions. *Journal of Sound and Vibration*. 143 (2), 241-253.

Langley, R. and Bremner, P. (1999). A hybrid method for the vibration analysis of a complex structural-acoustic system. *Journal of Acoustical Society of America*. 105(3).

Le Bot, A. and Cotoni, V. (2010). Validity diagrams of statistical energy analysis. *Journal of Sound and Vibration*. 329 (2010), 221-235.

Le Bot, A., Carbonelli, A. and Perrret-Liaudet. (2011). Entropy: A counterpart in Statistical Energy Analysis. *18th International Congress on Sound and Vibration*.

Lei, Y., Pan, J. and Sheng, M. (2012). Investigation of structural response and noise reduction of an acoustical enclosure using SEA method. *Applied Acoustics* 73 (2012), 348-355.

Lilly, J. (1987). Breakout in HVAC duct systems. *Sound and Vibration* 21(10).

Lyon, R. and DeJong, R. (1995). Theory and Application of Statistical Energy Analysis. *Butterworth-Heinemann, Newton, MA*.

Ming, R. and Pan, J. (2004). Insertion loss of an acoustic enclosure. *Journal of the Acoustical Society of America*. 116(6), 3453-3459.

Nikitin P.V., Stancil D.D. and Erosheva EA. (2011). Estimating the number of modes in multimodal waveguide propagation environment. *IEEE Symposium*. 1662-1665

Norton, M. (1999). Fundamentals of noise and vibration analysis for engineers. *Cambridge University Press, Cambridge*.

Price, A. and Crocker, M. (1970). Sound transmission through double panels using statistical energy analysis. *Journal of the Acoustical Society of America*. 47 (3), 683-693.

Ragnarsson, P., Pluymers B., Donders, S. and Desmet, W. (2010). Subcomponent modeling of input parameters for statistical energy analysis by using a wave-based boundary condition. *Journal of Sound and Vibration*. 329 (2010), 96-108.

Renji, K. and Nair, P. (2001). Non-Resonant response using statistical energy analysis. *Journal of Sound and Vibration*. 241(2), 253-270.

Rosa, S. (2010). On the use of the asymptotic scaled modal analysis for time-harmonic structural analysis and for the prediction of coupling loss factors for similar systems. Mechanical Systems and Signal Processing. 24(2010), 455-480.

Sarradj, E. (2004). Energy-based vibroacustics: SEA and beyond. Gesellschaft f'ur Akustikforschung Dresden mbH, D-01099 Dresden, Germany.

Sgard, F., Nelisse, H., Atalla, N., Amedin, C. and Oddo, R. (2010). Prediction of the acoustical performance of enclosure using a hybrid statistical energy analysis: Image source model. *Journal of the Acoustical Society of America*. 127(2), 784-795.

Shorter. P. (2007). The combination of statistical energy analysis and finite element analysis in the modeling of high frequency vibration. *Department of Mechanical Engineering, University of Auckland.*

Spah M. and Gibbs B. (2009). Reception plate method for characterization of structure-borne sound sources in buildings: assumptions and application. *Applied Acoustics*. 70, 361-368.

SS-EN 12354-1. (2000). Swedish institute for standards. *Stockholm, Sweden.*

Tang, S. (2005). Vibrational energy transmission through wall junctions in buildings. *Journal of Sound and Vibration*. 286 (2005), 1048-1056.

Thite, A. (2010). The effects of design modifications on the apparent coupling loss factors in SEA-like analysis. *Journal of Sound and Vibration*. 329 (2010), 5194-5208.

Ver, I. and Holmer, C. (1971). Noise and vibration control. *Leo Beranek (Ed.) McGraw-Hill, New York*. 287-296.

Wang, C., Lai, J.C.S. and Pulle, D.W.J. (2002). Prdiction of acoustic noise form variable speed induction motors: deterministic Vs statistical approaches. *Industry Applications, IEEE transcations*, 34(4), 1037-1044.

Woodhouse, J. (1981a). An introduction to statistical energy analysis of structural vibration. *Applied Acoustics*. 14, 455-469.

Woodhouse, J. (1981b). An approach to the theoretical background of statistical energy analysis applied to structural vibration. *Journal of the Acoustical Society of America*. 69(6)

Xie, G., Thompson, D. and Jones, C. (2005). The radiation efficiency of baffled plates and strips. *Journal of Sound and Vibration*. 280 (2005), 181-209.

Appendix A – MATLAB

```matlab
%%%%%%%%%%%%%%%%%%%%%%%%%%%
% Duct Design
%%%%%%%%%%%%%%%%%%%%%%%%%%%

% Input Parameters
fq = [63 125 250 500 1000 2000 4000 8000];
TL = zeros(length(fq), 1);
Lw6 = zeros(length(fq), 1);
W_c = zeros(length(fq), 1);
n1 = zeros(length(fq), 1);
P1 = 1;                                          % power in watts
c0 = 343;                                        % wave speed


for i = 1:length(fq)


f = fq(i);
omega = 2*pi*f;                                  % angular frequency




% Cavity 1 (Subsystem 1)
L1 = [0.305 0.610 6.1];
% dimensions in meters

S1 = 2*(L1(1)*L1(3)+L1(1)*L1(2)+L1(3)*L1(2));
% total surface area

V1 = prod(L1);
% volume

Le1 = 4*sum(L1);
% total edge length

Lv = 2*(L1(1)+L1(2));
% c/s duct perimeter


% Plate thickness [m]
h = 0.701e-3;


% Plate 1 (Subsystem 2)
L2 = [0.305 6.1 h];
G = 21e10;                                       % elasticity
mu = 0.3125;                                     % poissons ratio
rho = 7800;                                      % density (kg/m^3)
rhos = rho*L2(3);                                % density x thickness
S2 = L2(2)*L2(1);                                % surface area
Lp2 = 2*(L2(2)+L2(1));                           % perimeter
```

```matlab
% Plate 2 (Subsystem 3)
L3 = [0.610 6.1 h];
S3 = L3(1)*L3(2);
Lp3 = 2*(L3(1)+L3(2));



% Plate 3 (Subsystem 4)
L4 = [0.305 6.1 h];
S4 = L4(2)*L4(1);
Lp4 = 2*(L4(2)+L4(1));



% Plate 4 (Subsystem 5)
L5 = [0.610 6.1 h];
S5 = L5(1)*L5(2);
Lp5 = 2*(L5(1)+L5(2));



% Cavity 2 (Subsystem 6)
L6 = [700 400 300];
S6 = 2*(L6(1)*L6(2)+L6(1)*L6(3)+L6(2)*L6(3));
V6 = prod(L6);
Le6 = 4*sum(L6);                                    % total length




%%%%%%%%%%%%%%%%%%%%%%%%%%%%
% CACULATIONS
%%%%%%%%%%%%%%%%%%%%%%%%%%%%

gamma1 = 1.8e-4*sqrt(f);
eta11 = S1*c0*gamma1/(4*omega*V1);                 % total loss factor of sub 1


fc = sqrt(3*c0^4*rhos*(1-mu^2)/(pi^2*G*h^3));        % critical frequency

alpha = sqrt(f/fc);

 if f > fc
  sigma1 = (1-(fc/f))^(-1/2);
  sigma2 = (1-(fc/f))^(-1/2);

 elseif f == fc
   sigma1 = 0.45*sqrt((Lp2*fc)/c0);
   sigma2 = 0.45*sqrt((Lp3*fc)/c0);

 else
   sigma1 = (Lp2*c0/(4*pi^2*S2*fc))*(((1-alpha^2)*log((1+alpha)/(1-
alpha))+2*alpha)/(1-alpha^2)^(3/2));
```

```matlab
    sigma2 = (Lp3*c0/(4*pi^2*S3*fc))*(((1-alpha^2)*log((1+alpha)/(1-
alpha))+2*alpha)/(1-alpha^2)^(3/2));

 end




%%%%%%%%%%%%%%%%%%%%%%%%%%%%%%%%%%%%%%%%%%%%%%%%%%%%%%%%%%%%%%
% Coupling Loss Factors from the plate to cavity
%%%%%%%%%%%%%%%%%%%%%%%%%%%%%%%%%%%%%%%%%%%%%%%%%%%%%%%%%%%%%%

rho0 = 1.21;                                        % density of the air

if f >= fc

    eta21 = rho0*c0*sigma1/(omega*rhos);
    eta31 = rho0*c0*sigma2/(omega*rhos);
    eta41 = rho0*c0*sigma1/(omega*rhos);
    eta51 = rho0*c0*sigma2/(omega*rhos);


else
    eta21 = 2*rho0*c0*sigma1/(omega*rhos);
    eta31 = 2*rho0*c0*sigma2/(omega*rhos);
    eta41 = 2*rho0*c0*sigma1/(omega*rhos);
    eta51 = 2*rho0*c0*sigma2/(omega*rhos);


end




%%%%%%%%%%%%%%%%%%%%%%%%%%%%%%%%%%%%%%%%%%%%%%%
% Dissipation Factors of the plates
%%%%%%%%%%%%%%%%%%%%%%%%%%%%%%%%%%%%%%%%%%%%%%%


eta22 = (0.7/f^0.9);                                % total loss factor for sub 2
eta33 = (0.7/f^0.9);                                % total loss factor for sub 3
eta44 = (0.7/f^0.9);                                % total loss factor for sub 4
eta55 = (0.7/f^0.9);                                % total loss factor for sub 5


%%%%%%%%%%%%%%%%%%%%%%%%%%%%%%
% Lengths of connections
%%%%%%%%%%%%%%%%%%%%%%%%%%%%%%

L23 = L2(2);
L32 = L23;
L34 = L3(2);
L43 = L34;
L45 = L4(2);
```

```matlab
L54 = L45;
L52 = L5(2);
L25 = L52;



%%%%%%%%%%%%%%%%%%%%%%%%%%%%%%%%%%%%%%%%%%%
% Coupling Loss Factors between the plates
%%%%%%%%%%%%%%%%%%%%%%%%%%%%%%%%%%%%%%%%%%%


B = G*h^3/(12*(1-mu^2));

cB = (omega^2*B/rhos)^(1/4);

eta23 = 0.2068*cB*L23/(omega*S2);            % CLF within the sub 2 and sub 3

eta34 = 0.2068*cB*L34/(omega*S3);
eta45 = 0.2068*cB*L45/(omega*S4);
eta52 = 0.2068*cB*L52/(omega*S5);



%%%%%%%%%%%%%%%%%%%%%%%%%%%%%%%%%%%%%%%%%%%%%%%
% modal densities
%%%%%%%%%%%%%%%%%%%%%%%%%%%%%%%%%%%%%%%%%%%%%%%


n1(i) = (4*pi*f^2*V1/c0^3)+(pi*f*S1/(2*c0^2))+(Le1/(8*c0));
% modal density sub 1

cL = (G/(rho*(1-mu^2)))^(1/2);                     % longitudinal wave speed

n2 = sqrt(3)*S2/(cL*h);                     % modal densities of sub 2,3,4,5.
n3 = sqrt(3)*S3/(cL*h);
n4 = sqrt(3)*S4/(cL*h);
n5 = sqrt(3)*S5/(cL*h);



%%%%%%%%%%%%%%%%%%%%%%%%%%%%%%%%%%%%%%%%%%%%%%%%%%%%%%%%%%%%%%%%
% coupling loss factors related to modal densities
%%%%%%%%%%%%%%%%%%%%%%%%%%%%%%%%%%%%%%%%%%%%%%%%%%%%%%%%%%%%%%%%


eta12 = eta21*n2/n1(i);
eta13 = eta31*n3/n1(i);
eta14 = eta41*n4/n1(i);
eta15 = eta51*n5/n1(i);
eta32 = eta23*n2/n3;
eta43 = eta34*n3/n4;
eta54 = eta45*n4/n5;
eta25 = eta52*n5/n2;
```

```matlab
%%%%%%%%%%%%%%%%%%%%%%%%%%%%%%%%%%%%%%%%%%%
% Total Loss factors
%%%%%%%%%%%%%%%%%%%%%%%%%%%%%%%%%%%%%%%%%%%

eta1 = eta11;
eta2 = eta22+(eta21+eta23+eta25);
eta3 = eta33+(eta31+eta32+eta34);
eta4 = eta44+(eta41+eta43+eta45);
eta5 = eta55+(eta51+eta52+eta54);




%%%%%%%%%%%%%%%%%%%%%%%%%%%%%%%%%
% Transmission coefficients
%%%%%%%%%%%%%%%%%%%%%%%%%%%%%%%%%

R16 = 20*log10(f*rhos)-42;                          % Sound Reduction Index

tau16 = 1/(10^(R16/20));                            % Transmission Coefficient


%%%%%%%%%%%%%%%%%%%%%%%%%%%%%%%%%%%%%%%%%%%%%%%%%%%%%
% Non resonant Coupling Factor Cavity to Cavity
%%%%%%%%%%%%%%%%%%%%%%%%%%%%%%%%%%%%%%%%%%%%%%%%%%%%%

eta16 = 13.7*(S2+S3+S4+S5)*tau16/(f*V1);




%%%%%%%%%%%%%%%%%%%%%%%%%%%%%%%%%%%%%%%%%%%%%%%%%%%%%%%%%%%%%%%%%
% Matrix Formation
%%%%%%%%%%%%%%%%%%%%%%%%%%%%%%%%%%%%%%%%%%%%%%%%%%%%%%%%%%%%%%%%%

eta = [eta1 -eta21 -eta31 -eta41 -eta51;
       -eta12 eta2 -eta32 0 -eta52;
       -eta13 -eta23 eta3 -eta43 0;
       -eta14 0 -eta34 eta4 -eta54;
       -eta15 -eta25 0 -eta45 eta5];


W = [P1/omega 0 0 0 0].';

E = eta\W;

We = omega*eta1*E(1);        % sound power stored in the internal sound field



m2 = rho*(L2(2)*L2(1)*L2(3));                        % mass of the plates
m3 = rho*(L3(1)*L3(2)*L3(3));
m4 = rho*(L4(2)*L4(1)*L4(3));
m5 = rho*(L5(1)*L5(2)*L5(3));
```

```matlab
v2 = sqrt(E(2)/m2);                               % Average Vibration Velocity
v3 = sqrt(E(3)/m3);
v4 = sqrt(E(4)/m4);
v5 = sqrt(E(5)/m5);



Wr = rho0*c0*(S2*sigma1*v2^2 + S3*sigma2*v3^2 + S4*sigma1*v4^2 +
S5*sigma2*v5^2);                                            % Resonant Power

W_non = P1*tau16;                                       % Non-resonant Power

W_c(i) = Wr + W_non;             % Total sound power radiated from an enclosure


Lw6(i) = 10*log10(W_c(i)/10^-12);                   % Power Level out in Sub 6

Lw1 = 10*log10(We/10^-12);                          % Power Level in the duct

alpha = [1.31 0.66 0.33 0.16 0.16 0.16 0.16 0.16];      % duct attenuation

gamma = 10^(-alpha(i)/10);

EL = (gamma^L1(3)-1)/(log(gamma));                       % Effective Length


ES = Lv*EL;                                         % Effective Surface Area


csa = L1(1)*L1(2);                      % cross sectional area inside of duct



%%%%%%%%%%%%%%%%%%%%%%%%%%%%%%%%%%%%%%%%%%%%%%%%%%%%%%%%%%%%%%
% Calculating the Transmission Loss
%%%%%%%%%%%%%%%%%%%%%%%%%%%%%%%%%%%%%%%%%%%%%%%%%%%%%%%%%%%%%%


TL(i) =(Lw1 - Lw6(i) + 10*log10(ES/csa));


w_t = 30*c0/(L1(1) + L1(2));

f_t = w_t/2/pi;                                         % transition frequency
```

```matlab
if f > f_t

    F = f*(L1(1) + L1(2))/(30*c0*2*pi);

    TL(i) = TL(i) + 10*log10(2*pi*f*(L1(1) + L1(2))/30/c0);

% applying the correction factor

    end

end
```